Chapter 7
Drug-Based Network Pharmacology Practice Process

Xiaobo Sun, Xiaoyan Xing, and Min Wang

7.1 Guide to this Chapter

TCM has a long history and notable therapeutic effect in China [1, 2]. Starting from the holistic and systematic of drug–target–disease interactions, network pharmacology employs complex network models to enunciate and scrutinize drug–target–disease network relationships [3]. The holistic and methodical characteristics of network pharmacology coincide with the holistic view of TCM theory and the principle of syndrome differentiation and treatment, which provides new ideas and perspectives for the systematic research of TCM [4].

Considering the classic and reputed Guanxin Danshen Formulation and the commonly used Chinese medicines Ginseng Radix et Rhizoma, Notoginseng Radix et Rhizoma, and Salviae miltiorrhizae Radix et Rhizoma as examples, this chapter introduces the practice process of network pharmacology based on drugs from six aspects: active ingredients identification, mechanism analysis, compatibility theory of TCM, interaction between Chinese and Western medicines, drug repurposing, and multi-targets drug development, and attempts to provide clues with reference value for the application of network pharmacology in TCM research.

X. Sun (✉) · X. Xing · M. Wang
Institute of Medicinal Plant Development, Chinese Academy of Medical Sciences and Peking Union Medical College, Beijing, China

S. Li (ed.), *Network Pharmacology*, https://doi.org/10.1007/978-981-16-0753-0_7

7.2 Finding the Active Ingredients of a Single Chinese Medicine or Prescription

Indefinite material basis and indefinite mechanism of action are the salient hurdles to the wider acceptance of TCM in the international community. Therefore, the identification of active ingredients in TCM is a crucial challenge to be decoded in the modernization of traditional Chinese medicine. The typical measures for network pharmacology to identify the effective ingredients of TCM are as follows: Primarily, the information related to chemical components, chemical component targets, and disease targets of TCM are collated based on database retrieval and computer simulation technology. Subsequently, these data are taken as nodes in the network, and the "TCM–component" network, the "component–target" network, and the "disease–gene" network are constructed based on the interconnection between the nodes. Finally, the overall "TCM–component–target–disease" network is fabricated by a network composite. The interconnection between the elements is scrutinized based on the overall network, in order to detect the potential effective component group of TCM for the treatment of specific diseases.

Guanxin Danshen Formulation (GXDSF) is a classic prescription commonly used in clinical practice. It consists of three Chinese herbs: Salvia miltiorrhiza, Panax notoginseng, and Dalbergia odorifera oil. It is effective in improving blood circulation and disperse stasis, regulating qi and relieving pain. It is predominantly used in the treatment of coronary heart disease with qi stagnation and blood stasis. Modern compound preparations developed on the basis of GXDSF, such as Guanxin Danshen tablet, Guanxin Danshen capsule, and Guanxin Danshen dripping pills, have significant clinical efficacy and are widely used in the prevention and treatment of coronary heart disease [5]. Expounding the active ingredient basis of GXDSF can provide expedient clues for the R&D of new drugs in the treatment of cardiovascular disease (CVD). Therefore, case in point of GXDSF, identifying the effective component groups of TCM prescriptions based on network pharmacology is introduced exhaustively below. The research flow is as demonstrated in Fig. 7.1.

7.2.1 Data Acquisition and Processing

7.2.1.1 Chemical Component Collection of Complete GXDSF Prescription

The chemical components of the complete GXDSF prescription were assembled based on two classic Chinese herbal medicine databases—ETCM and TCM-MESH. The "Herbs" option was selected under the MENU option of the ETCM database menu bar, and "Salvia miltiorrhiza" was entered in the search box to obtain the chemical composition list 1 of radix Salviae Miltiorrhizae. "Herb" was selected under the Search Type option of TCM-MESH database, "Pinyin name" was selected

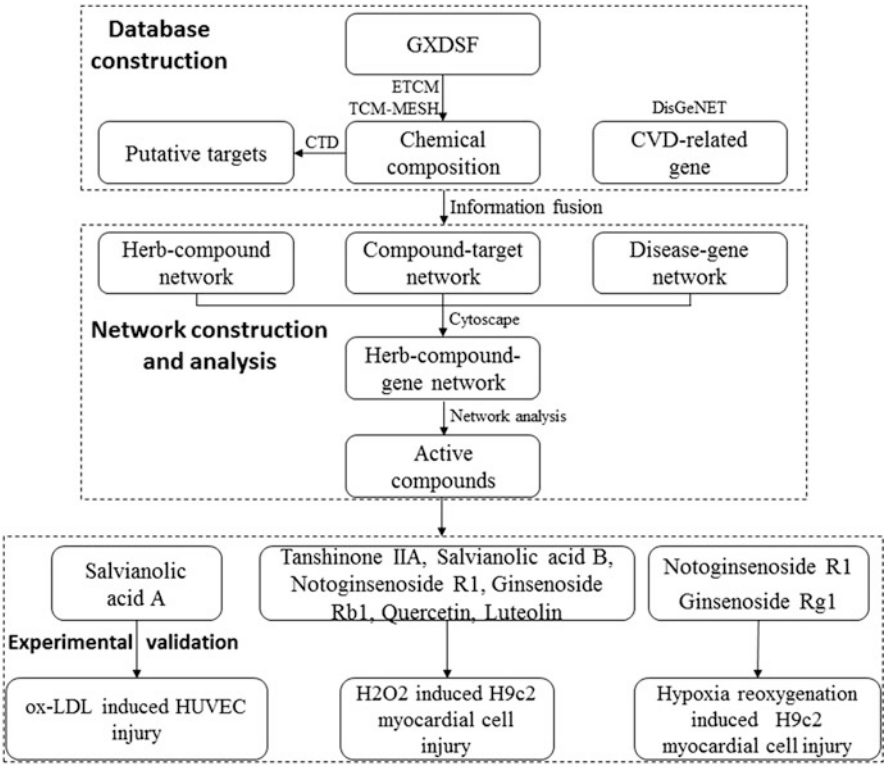

Fig. 7.1 Research ideas and processes

under Herb Name Type option, and "Dan Shen" entered in the search box to obtain the chemical composition list two of radix Salviae Miltiorrhizae. The two chemical component lists of Danshen assembled based on the ETCM and TCM-MESH databases were integrated and deduplication processing was performed to obtain a complete chemical component list of Salvia miltiorrhiza medicinal materials. The chemical components of the two medicinal materials of Panax notoginseng and Dalbergia odorifera were assembled using the same method. The corresponding relationship between each Chinese medicine and its chemical composition was saved in the form of a two-dimensional table.

7.2.1.2 Collection of Chemical Component Targets

The "Chemicals" option was selected under the Keyword Search option of the CTD database, the appropriate English name of each chemical component was entered in the search box, and the target data of each chemical component was assembled. The corresponding relationship between each chemical component and its target was saved in the form of a two-dimensional table. The mass search function provided by

the CTD database can also be used to retrieve the target data of each chemical component.

7.2.1.3 Collection of CVD-Related Disease Genes

The "Search" option was selected in the menu bar of the DisGeNET database, the search type was set to "diseases," and cardiovascular disease was entered in the search box, to assemble the CVD-related target gene data. The corresponding relationship between the disease and its related genes was saved in the form of a two-dimensional table.

7.2.2 Network Construction and Visualization

The "TCM–ingredient" list, "ingredient–target" list, and "disease–gene" list obtained in the data source were entered into Cytoscape 3.5.0 network analysis and visualization software. The merge function under the "Tools" option in the menu bar was used to superimpose networks to construct a "TCM–ingredient–disease–target" network. To increase the self-evidence of the network, different attributes (shape, size, color, font, etc.) can be set for different nodes in the network. At the same time, the visualization effect of the network can be adjusted through the network layout function under the "Layout" option in the menu bar.

The Network Analyzer function under the "Tools" option in the Cytoscape 3.5.0 menu bar was used to analyze the topological attributes (connectivity) of each node in the network.

7.2.3 Network Analysis and Prediction

7.2.3.1 Chemical Components of Complete GXDSF Prescription and Its Targets

Based on the ETCM and TCM-MESH database, there are a total of 115 chemical components of Salvia miltiorrhiza, 121 chemical components of Panax notoginseng, and 35 chemical components of Dalbergia odorifera assembled in this study. By means of chemical component deduplication treatment, a total of 267 chemical components of Complete GXDSF Prescription are collected. The number of chemical component targets corresponding to Salvia miltiorrhiza, Panax notoginseng, Dalbergia odorifera, and GXDSF is 241, 215, 101, and 398, respectively (as shown in Table 7.1). The Venn diagram distribution shows that there are pronounced differences in the chemical composition of the three medicinal materials of salvia miltiorrhiza, Panax notoginseng, and Dalbergia odorifera (As shown in Fig. 7.2).

Table 7.1 Chemical components of complete GXDSF prescription and its targets

Data type	Traditional Chinese medicine			Total
	Salvia miltiorrhiza	Panax notoginseng	Dalbergia odorifera	
Chemical composition	115	121	35	267
Targets	241	215	101	398

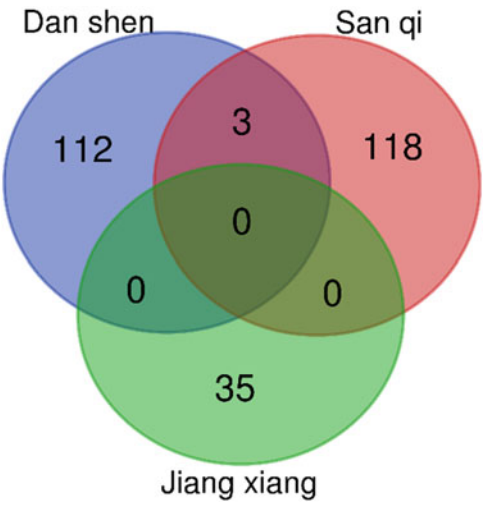

Fig. 7.2 Venn diagram—chemical composition of GXDSF

7.2.3.2 Analysis of TCM–Ingredient–Disease Target Network

Figure 7.3 shows the TCM–component–disease target network of GXDSF for CVD treatment. As demonstrated in Fig. 7.3, the three traditional Chinese medicines Salvia miltiorrhiza, Panax notoginseng, and Dalbergia odorifera have certain regulatory effects on CVD-related genes. A total of 37 ingredients in GXDSF are associated in the regulation of CVD. Among them, 21 ingredients are from Salvia miltiorrhiza, 2 ingredients are from Dalbergia odorifera, and 16 ingredients are from Panax notoginseng. The results confirm that Salvia miltiorrhiza, Dalbergia odorifera, and Panax notoginseng execute a synergistic role in the treatment of CVD by means of distinct active components.

Yellow, green, and red round nodes represent TCM, TCM chemical components, and disease targets, respectively. The size of each node is adjusted according to the topology parameter—connectivity of nodes in the network. The larger the node, the greater the connectivity of the node in the network, and vice versa. The size of the node reflects the importance of the node in the network to a certain extent. The gray edge represents the inclusive or regulating relationship between the two nodes.

By and large, kaempferol, luteolin, palmitic acid, tanshinone IIB, tanshinone IIA, tanshinone I, and other ingredients, together totaling 37 ingredients, constitute the effective ingredient group of GXDSF that plays a synergistic role in the treatment of CVD. Table 7.2 shows the source, English name, Chinese name, CAS number, and

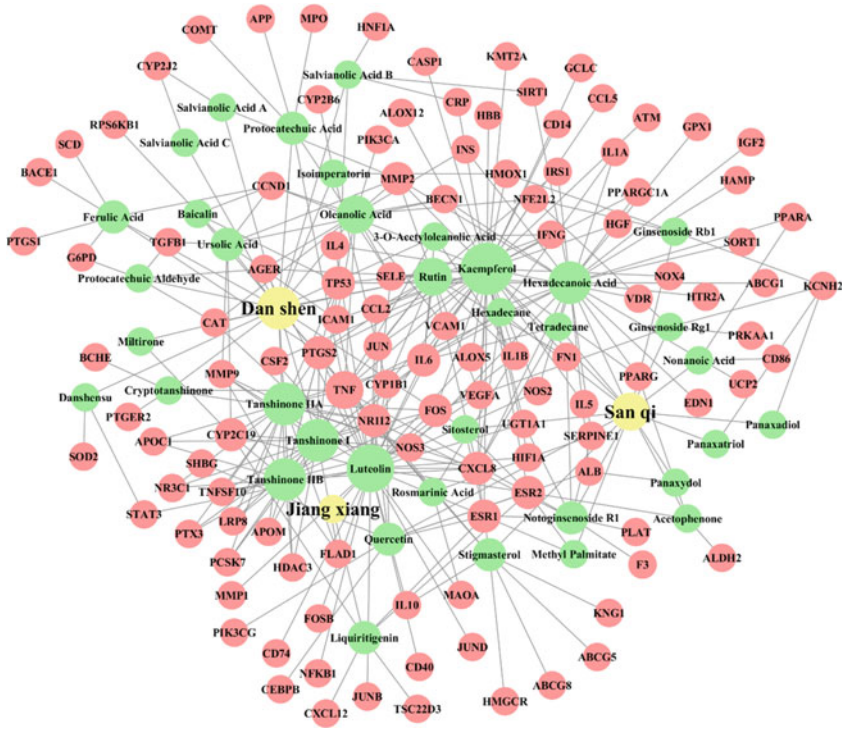

Fig. 7.3 TCM–component–disease target network

topological parameter information of each component in the GXDSF effective ingredient group.

7.2.4 Verification and Summary

Integrating the content of each chemical component in the medicinal components and its topological parameter—connectivity in the network, we hand-picked nine components (Kaempferol, luteolin, tanshinone IIA, quercetin, Notoginsenoside R1, salvianolic acid B, Ginsenoside Rg1, ginsenoside Rb1, and salvianolic acid A) from the above 37 to verify the activity of cardiovascular protection.

Through experiments, we verified that (1) Protective effects of tanshinone IIA, salvianolic acid B, Notoginsenoside R1, ginsenoside Rb_1, quercetin, and luteolin on H_2O_2 induced H9c2 myocardial cell injury; (2) Protective effects of Notoginsenoside R1 and ginsenoside Rg1 on H9c2 cardiomyocytes injury were induced by hypoxia reoxygenation; (3) Protective effects of salvianolic acid A on oxidative low-density lipoprotein (ox-LDL) induced injury of human umbilical vein endothelial cells; (4) Protective effects of kaempferol on doxorubicin-induced H9c2

Table 7.2 Effective component group of GXDSF

Serial No.	Source of medicinal materials	Chemical compound	Chinese name	CAS	Connectivity
1	Panax notoginseng	Kaempferol	Kaempferol	520-18-3	44
2	Dalbergia odorifera	Luteolin	Luteolin	491-70-3	36
3	Panax notoginseng	Hexadecanoic acid	Palmitic acid	1957-10-3	26
4	Salvia miltiorrhiza	Tanshinone IIb	Tanshinone IIB	17397-93-2	19
5	Salvia miltiorrhiza	Tanshinone IIa	Tanshinone IIA	568-72-9	19
6	Salvia miltiorrhiza	Tanshinone I	Tanshinone I	568-73-0	19
7	Salvia miltiorrhiza	Rutin	Rutin	153-18-4	15
8	Salvia miltiorrhiza	Oleanolic acid	Oleanolic acid	508-02-1	12
9	Panax notoginseng	Quercetin	Quercetin	117-39-5	8
10	Salvia miltiorrhiza	Ursolic acid	Ursolic acid	77-52-1	8
11	Panax notoginseng	Notoginsenoside R1	Notoginsenoside R1	80418-24-2	8
12	Salvia miltiorrhiza, Panax notoginseng	Stigmasterol	Stigmasterol	83-48-7	7
13	Salvia miltiorrhiza	Ferulic acid	Ferulic acid	1135-24-6	6
14	Salvia miltiorrhiza	Protocatechuic acid	Protocatechuic acid	99-50-3	5
15	Dalbergia odorifera	Liquiritigenin	Liquiritigenin	578-86-9	5
16	Salvia miltiorrhiza	Salvianolic acid B	Salvianolic acid B	115939-25-8	4
17	Salvia miltiorrhiza	Protocatechuic aldehyde	Protocatechuic aldehyde	139-85-5	4
18	Panax notoginseng	Ginsenoside Rg1	Ginsenoside Rg1	22427-39-0	4
19	Salvia miltiorrhiza	Cryptotanshinone	Cryptotanshinone	35825-57-1	4
20	Salvia miltiorrhiza	3-O-Acetyloleanolic acid	Oleanolic acid 3-acetate	4339-72-4	4
21	Salvia miltiorrhiza	Rosmarinic acid	Rosmarinic acid	537-15-5	4
22	Panax notoginseng	Hexadecane	N-hexadecane	544-76-3	3
23	Panax notoginseng	Tetradecane	N-tetradecane	629-59-4	3
24	Panax notoginseng	Acetophenone	Acetophenone	98-86-2	3

(continued)

Table 7.2 (continued)

Serial No.	Source of medicinal materials	Chemical compound	Chinese name	CAS	Connectivity
25	Panax notoginseng	Ginsenoside Rb1	Ginsenoside Rb1	41753-43-9	3
26	Salvia miltiorrhiza	Isoimperatorin	Isoimperatorin	482-45-1	3
27	Panax notoginseng	Nonanoic acid	Nonanoic acid	112-05-0	2
28	Panax notoginseng	Methyl palmitate	Methyl palmitate	112-39-0	2
29	Salvia miltiorrhiza	Baicalin	Baicalin	21967-41-9	2
30	Salvia miltiorrhiza	Danshensu	Tanshinol	23028-17-3	2
31	Salvia miltiorrhiza	Salvianolic acid A	Salvianolic acid A	96574-01-5	2
32	Salvia miltiorrhiza, Panax notoginseng	Sitosterol	β-sitosterol	83-46-5	2
33	Panax notoginseng	Panaxadiol	Panaxadiol	19666-76-3	1
34	Salvia miltiorrhiza	Miltirone	Miltirone	27210-57-7	1
35	Panax notoginseng	Panaxatriol	Panaxatriol	32791-84-7	1
36	Panax notoginseng	Panaxydol	Panaxydol	72800-72-7	1
37	Salvia miltiorrhiza	Salvianolic acid C	Salvianolic acid C	115841-09-3	1

cardiomyocyte injury. By and large, the effective component group of GXDSF was identified by using the network pharmacology method, and the cardiovascular protective effects of some components were verified by different in vitro cell models. The results of network analysis are highly consistent with the experimental results, which signify that network pharmacology is an effective means to identify the material basis of traditional Chinese medicines/TCM compound prescriptions.

7.2.4.1 Effects of Tanshinone IIA, Salvianolic Acid B, Notoginsenoside R1, Ginsenoside Rb_1, Quercetin, and Luteolin on H_2O_2 Induced H9c2 Myocardial Cell Injury; Protective Effect of H_2O_2 on H9c2 Myocardial Cell Injury

After pre-incubating different concentrations of tanshinone IIA, salvianolic acid B, notoginsenoside R1, ginsenoside Rb1, and luteolin for a corresponding time, 150 μM H_2O_2 was allowed to react for 6 h. The MTT method was employed to detect the consequences of each active ingredient on H9c2 myocardial cell activity.

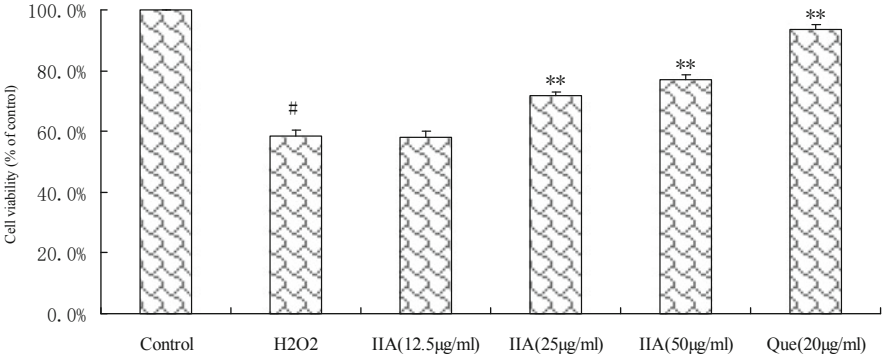

Fig. 7.4 Effect of tanshinone IIA on H_2O_2-induced H9c2 myocardial cell injury. *IIA* tanshinone IIA, *Que* quercetin, $^{\#}P < 0.01$ (model group vs control group), $^{**}P < 0.01$ (processing group vs model group)

The results demonstrate that: Tanshinone IIA, a fat-soluble component of Salvia miltiorrhiza, exhibits significant myocardial cell protective effect at 50 μg/ml and 25 μg/ml (as shown in Fig. 7.4). Salvianolic acid B, a water-soluble component, has protective effects on myocardial cells at 12.5 μg/ml and 6.25 μg/ml (as shown in Fig. 7.5). Ginsenoside Rb1 in Panax notoginseng has a significant inhibitory effect on H_2O_2-induced decline in myocardial cell activity at 50 μg/ml and 25 μg/ml (as shown in Fig. 7.6). However, notoginsenoside R1 has no significant effect on H_2O_2-induced H9c2 cell damage within the detection concentration range (3.125–200 μg/ml) (as shown in Fig. 7.7). Luteolin, a flavonoid from Dalbergia odorifera, has significant protective effects on myocardial cells. The cardiomyocyte activity in the model group is 52.7%±1.1% of that in the normal group, while that in the luteolin 12.5 μg/ml and 25 μg/ml pre-incubation groups are 81.9%±1.4% and 89.2%±1.4%, respectively. The cardiomyocyte activity in the luteolin group is significantly higher than that in the model group (as shown in Fig. 7.8). Quercetin shows significant protective effects on myocardial cells at concentrations of 20 μg/ml and 40 μg/ml. In the same dose, its protective effect on myocardial cells is significantly higher than that of tanshinone IIA, ginsenoside Rb1, and notoginsenoside R1 (as shown in Figs. 7.4, 7.6, and 7.7).

7.2.4.2 Protective Effects of Notoginsenoside R1 and Ginsenoside Rg1 on H9c2 Myocardial Cell Injury Induced by Hypoxia Reoxygenation

After pre-incubation with different concentrations of notoginsenoside R1 and ginsenoside Rg1 for a corresponding time, hypoxia reoxygenation damage occurred on myocardial cells. The CCK-8 method was employed to detect the activity of myocardial cells. Compared to the control group, the survival rate of H9c2 cells was significantly reduced due to 6 h of hypoxia and 12 h of reoxygenation. After

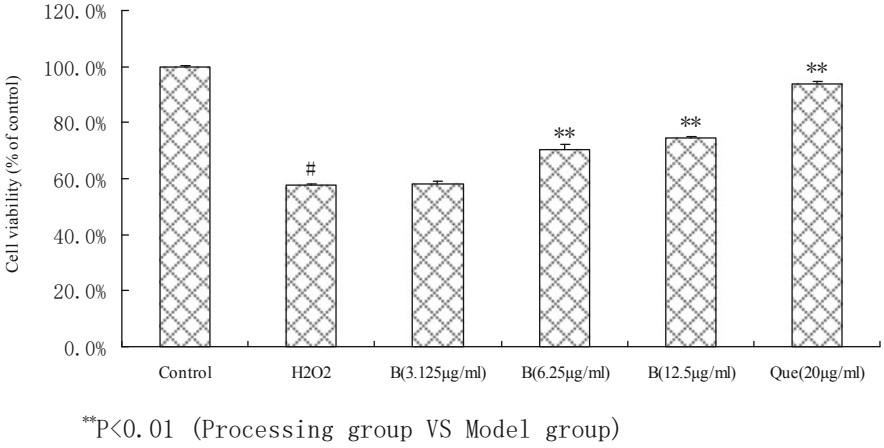

Fig. 7.5 Effect of salvianolic acid B on H_2O_2-induced H9c2 myocardial cell injury. *B* salvianolic acid B, *Que* quercetin, $^{\#}P < 0.01$ (model group vs control group), $^{**}P < 0.01$ (processing group vs model group)

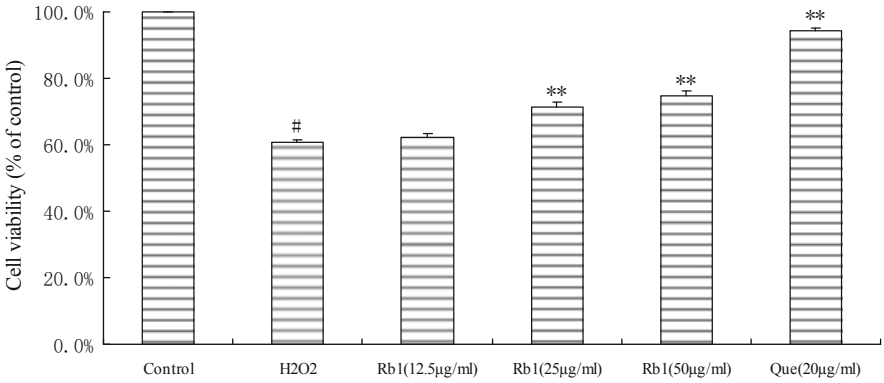

Fig. 7.6 Effects of ginsenoside Rb1 on H_2O_2-induced H9c2 myocardial cell injury. *Rb1* ginsenoside Rb1, *Que* quercetin, $^{\#}P < 0.01$ (model group vs control group), $^{**}P < 0.01$ (processing group vs model group)

pre-incubation with different concentrations of notoginsenoside R1 and ginsenoside Rg1 (2.5, 5, 10, 20, 40, 80 μmol/L) for 24 h, they all demonstrated sublime cell protective effects, and significantly enhanced the cell survival rate, demonstrating a dose-dependent trend (as shown in Fig. 7.9).

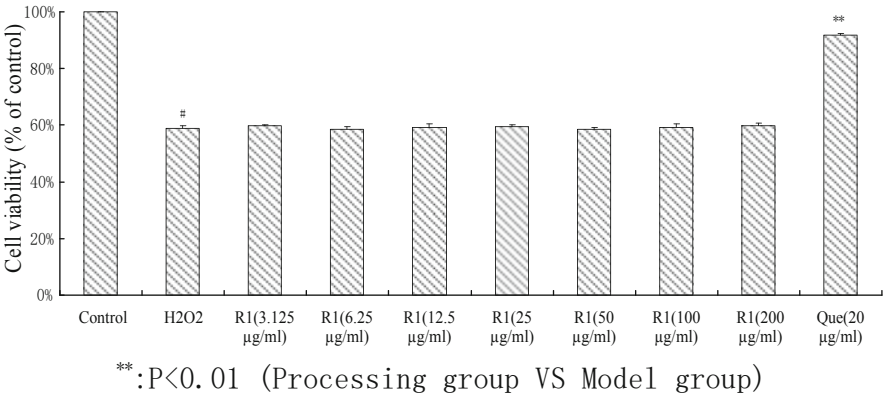

Fig. 7.7 Effects of notoginsenoside R1 on H_2O_2-induced H9c2 myocardial cell injury. *R1* notoginsenoside R1, *Que* quercetin, $^{\#}P < 0.01$ (model group vs control group), $^{**}P < 0.01$ (processing group vs model group)

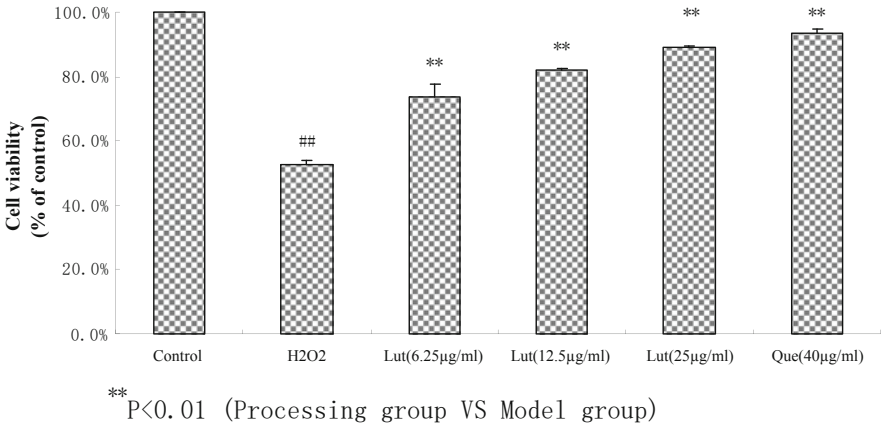

Fig. 7.8 Effects of luteolin on H_2O_2-induced H9c2 myocardial cell injury. *Lut* luteolin, *Que* quercetin, $^{\#\#}P < 0.01$ (model group vs control group), $^{**}P < 0.01$ (Processing group vs model group)

7.2.4.3 Protective Effects of Salvianolic Acid A on ox-LDL-Induced Injury of Human Umbilical Vein Endothelial Cells

After 12 h pre-incubation with different concentrations of salvianolic acid A, 70 μg/ml ox-LDL was allowed to react for 24 h. The CCK-8 method was employed to detect the activity of cells. The results demonstrate that salvianolic acid A protects ox-LDL-induced injury to human umbilical vein endothelial cells, in acceptable doses. At the outset, the effective concentration of salvianolic acid A is low, and it significantly reduce the ox-LDL-induced injury to human umbilical vein endothelial

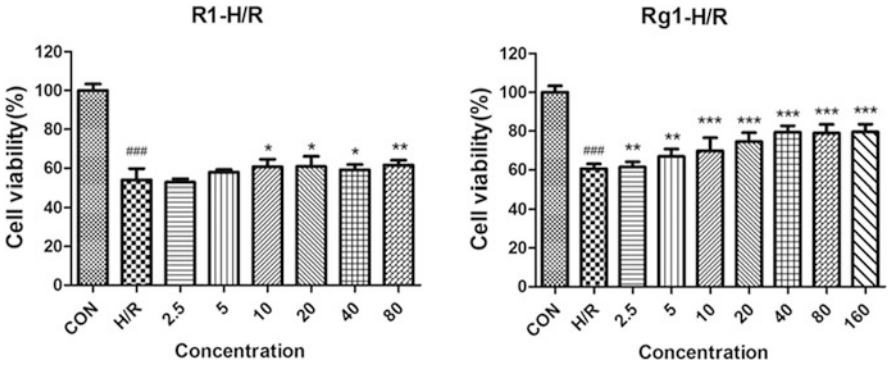

Fig. 7.9 Effects of notoginsenoside R1 and ginsenoside Rg1 on H9c2 myocardial cell injury induced by hypoxia reoxygenation. *R1* notoginsenoside R1, *Rg1* ginsenoside Rg1. $^{\#\#\#}P < 0.001$ (model group vs control group), $^{*}P < 0.05$ (processing group vs model group), $^{**}P < 0.01$ (processing group vs model group), $^{***}P < 0.001$ (processing group vs model group)

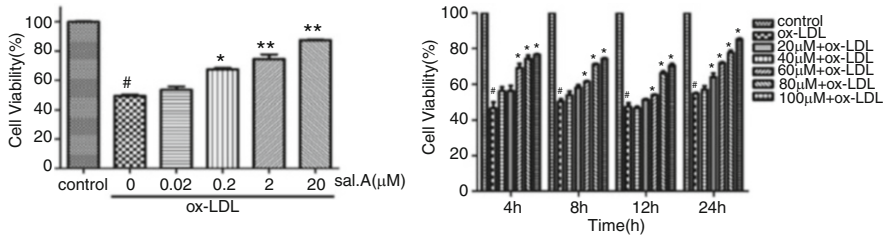

Fig. 7.10 Effect of salvianolic acid A on ox-LDL-induced injury of human umbilical vein endothelial cells. *Sal.A* salvianolic acid A, $^{\#}P < 0.001$ (model group vs control group), $^{*}P < 0.05$ (processing group vs model group), $^{**}P < 0.01$ (processing group vs model group)

cell at a concentration of 0.2 μm. However, salvianolic acid A shows obvious cytotoxic effects at concentrations above 25 μmol (as shown in Fig. 7.10).

7.2.4.4 Protective Effects of Kaempferol on h9c2 Cardiomyocyte Injury Induced by Doxorubicin

After 24 h pre-incubation with different concentrations of kaempferol, 1 μM doxorubicin was allowed to react for 4 h. The MTT method was employed to detect the effects of different concentrations of kaempferol on H9c2 myocardial cell activity. The results demonstrate that kaempferol at different concentrations significantly reduced the doxorubicin-induced H9c2 cardiomyocyte injury (as shown in Fig. 7.11).

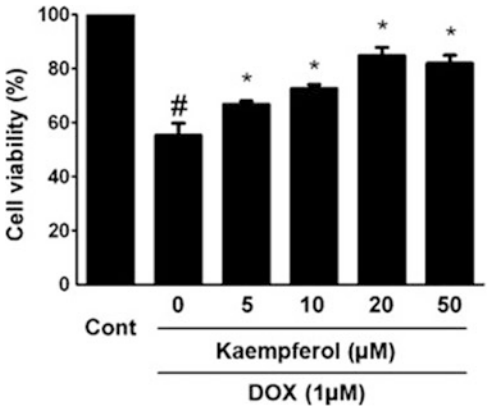

Fig. 7.11 Effect of kaempferol on doxorubicin-induced H9c2 cardiomyocyte injury. $^{\#}P < 0.05$ (model group vs control group), $^{**}P < 0.05$ (processing group vs model group)

7.2.4.5 Summary

Taking Guanxin Danshen Formulation (GXDSF), a classic and famous prescription as an example, this section exhaustively introduces the experimental reasoning and measures of identifying the effective component groups of TCM/TCM compound prescriptions based on the network pharmacology method, in an attempt to provide reference for the application of network pharmacology in the research of the component basis of TCM/TCM compound prescriptions. Contingent on ETCM, TCM-MESH, CTD, and DisGeNET databases, this section constructs a TCM–ingredient–disease target network of GXDSF in the treatment of CVD diseases based on the network pharmacology method. By means of network analysis, we identified 37 monomer chemical components, which collectively constitute the active component group of GXDSF. Based on the component of each chemical component in the medicinal ingredients and its topological parameter—connectivity in the network, we hand-picked 9 components (kaempferol, luteolin, tanshinone IIA, quercetin, Notoginsenoside R1, salvianolic acid B, Ginsenoside Rg1, ginsenoside Rb1, and salvianolic acid A) from the above 37 to verify the activity of cardiovascular protection. The results demonstrate that tanshinone IIA, salvianolic acid B, ginsenoside Rb1, quercetin, and luteolin have protective effects on H_2O_2-induced H9c2 myocardial cell injury. Ginsenoside Rg1 has protective effect on H9c2 myocardial cell injury induced by anoxic reoxygenation. Albeit notoginsenoside R1 has no significant consequence on H_2O_2-induced H9c2 cell injury, it could significantly enhance H9c2 myocardial cell injury induced by hypoxia reoxygenation. Different concentrations of kaempferol can significantly enhance doxorubicin-induced H9c2 myocardial cell injury. Based on the ox-LDL-induced injury model of human umbilical vein endothelial cells, we verified the effect of salvianolic acid A pretreatment on cell activity. The results demonstrate that salvianolic acid A can protect ox-LDL-induced human umbilical vein endothelial cells from damage in a dose-dependent manner. By and large, we detected the effective component group of GXDSF based on the network pharmacology method, and the cardiovascular

protective effects of some components were verified by different in vitro cell models. The results of network analysis have high consistency with the experimental results, which signifies that network pharmacology is an effective means to identify the material basis of traditional Chinese medicines/TCM compound prescriptions.

7.3 Expounding the Pharmacodynamic Mechanism of Single Chinese Medicine or Prescription

Traditional Chinese medicine and TCM prescriptions have multi-component, multi-target, and multi-pathway functional characteristics, and have significant advantages in the treatment of complex diseases. Traditional research procedures predominantly employ phytochemical separation, extraction, identification, and other technologies to explore the primary effective components in TCM or compound prescriptions, and subsequently employ modern pharmacological means to investigate the primary action target and signaling pathway, as a means to explore its mechanism of action. However, this "single target–single component" chemical drug development model is inconsistent with the application of synergistic compatibility of TCM and their compounds, and cannot comprehensively explain the clinical effect of TCM and its compound prescription. The emergence of network pharmacology promotes the discovery, research, and development of drugs and the elucidation of therapeutic mechanism [6], providing a new research idea and method for TCM and its compounds [7–9].

Guanxin Danshen Formulation is a classic compound prescription composed of Salvia miltiorrhiza, Panax notoginseng, and Dalbergia odorifera oil. In the preceding research of its protective effect on Ischemia-Reperfusion Injury-Induced Left Myocardial Ventricular Remodeling (MIRI-LVR), the author discovered that Guanxin Danshen Formulation can enhance the cardiac systolic function of MIRI-LVR model rats in acceptable doses, and demonstrates a significant inhibitory effect on MIRI-LVR, however, its mechanism of action is not comprehensible. Although the pharmacological action and mechanism of action of certain chemical components in Guanxin Danshen Formulation have been researched and documented, the joint action mechanism of several complex components in the compound cannot be validated. In this section, we employ the network pharmacology method to predict the possible action targets and mechanism of action of Guanxin Danshen Formulation on MIRI-LVR, providing research ideas for elucidating the complex mechanism of action of TCM compounds.

7.3.1 Data Acquisition and Processing

The research ideas and processes are shown in Fig. 7.12.

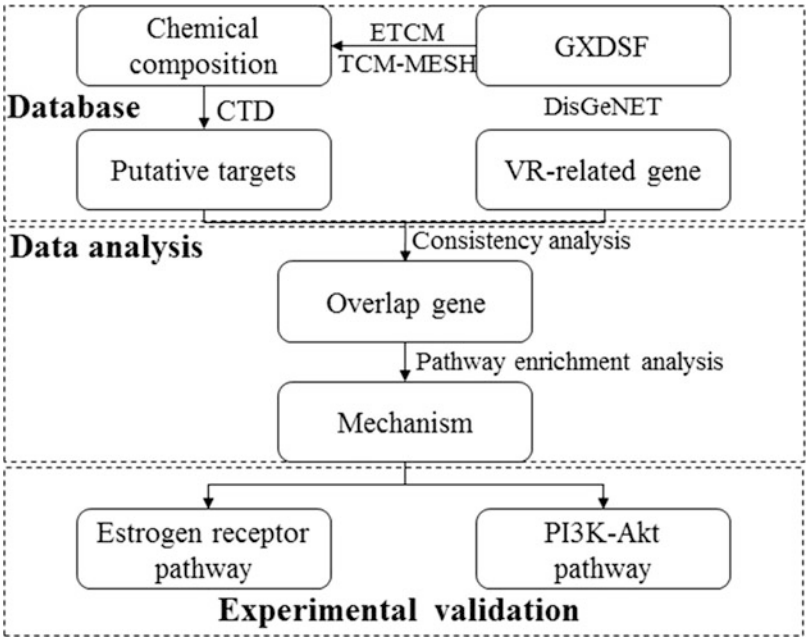

Fig. 7.12 Research ideas and processes

7.3.1.1 Chemical Component Collection of GXDSF Prescription

Based on two classic Chinese herbal medicine databases, ETCM and TCM-MESH, the chemical ingredients of GXDSF prescription were assembled. (1) The "Herbs" option is selected under the MENU option in the ETCM database menu bar, and "danshen" is entered in the search box, to obtain chemical composition list 1 of Radix Salviae Miltiorrhizae. (2) "Herb" is selected under the Search Type option in the TCM-MESH database, the "Pinyin Name" option is selected under Herb Name Type option, and "Dan Shen" is entered in the search box to get the chemical composition list 2 of Radix Salviae Miltiorrhizae. (3) The two chemical composition lists of Salviae Miltiorrhizae collected based on ETCM and TCM-MESH databases are integrated and de-duplicated, creating the complete chemical composition list of Radix Salviae Miltiorrhizae. (4) The chemical components of panax notoginseng and dalbergia odorifera are assembled employing the same method. The corresponding relationship between each traditional Chinese medicine and its chemical components are saved in the form of a two-dimensional list.

7.3.1.2 Collection of Chemical Component Targets

The "Chemicals" option was selected under Keyword Search in the CTD database and the English name of each chemical component was entered in the search box, to

assemble the target data of each chemical component. The corresponding relationship between each chemical component and its target was saved in the form of a two-dimensional list. The mass search function provided by the CTD database can also be employed to retrieve the target data of each chemical component.

7.3.1.3 Collection of VR-Related Disease Genes

The "Search" option was selected under the menu bar in the CTD database, the search type was set to "diseases," and Ventricular remodeling was entered in the search box to assemble the top 100 VR-related genes in the Inference Score. The corresponding relationship between the disease and its related genes was saved in the form of a two-dimensional list.

7.3.2 Network Construction and Visualization

7.3.2.1 Pathway Enrichment Analysis

The "set analyzer" option was selected under the "analyze" option in the CTD database, Genes was selected as the input type, and the abbreviation of the target gene entered in the input box. "Enriched pathways" was selected as the analysis type, and the corrected P-value threshold value was set to 0.001.

7.3.2.2 TCM–Target Network

The corresponding relationships between various TCM and VR-related genes in GXDSF were saved in the form of a two-dimensional list. Cytoscape 3.5.0 software was used to realize the visualization of the TCM–target network.

The NetworkAnalyzer function under the "Tools" option under the menu bar in Cytoscape 3.5.0 was employed to analyze the topology attributes (connectivity) of each node in the network.

7.3.3 Network Analysis and Prediction

7.3.3.1 Coincidence Degree Between GXDSF Component Target Proteins and VR-Related Genes

By implementing the consistency analysis of the chemical composition target proteins of the complete GXDSF prescription and VR-related genes, it was established that a total of 56 target proteins in GXDSF appear in the list of VR-related genes,

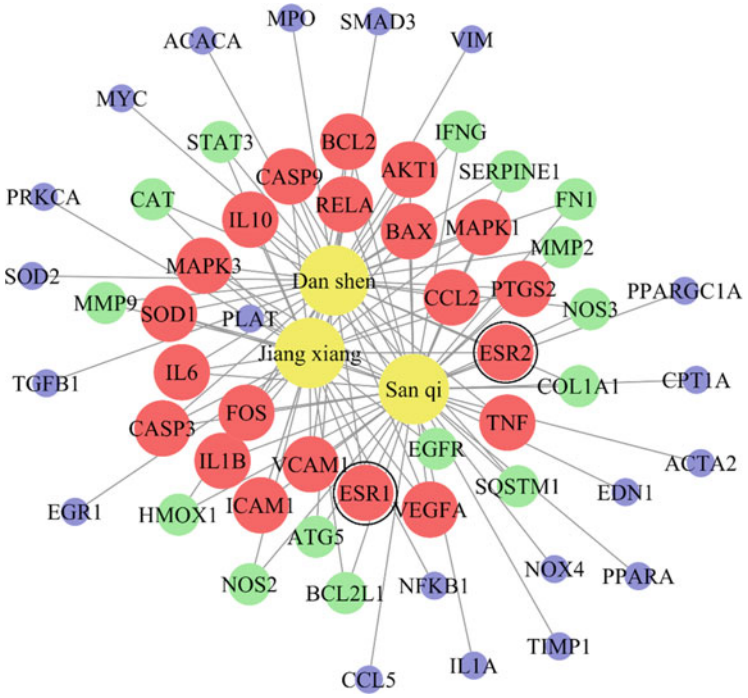

Fig. 7.13 TCM–target network of GXDSF in the treatment of VR. The yellow square nodes represent TCM. The red, green, and blue circular nodes represent VR-related genes with connectivity degrees 1, 2, and 3, respectively. The size of connectivity represents the number of Chinese medicines involved in the regulation of this gene in GXDSF. The genes in black circles are ESR1 and ESR2

accounting for 56% (56/100) of all VR-related genes. GXDSF may achieve direct regulation of VR by means of these target proteins.

7.3.3.2 TCM–Target Network of GXDSF in the Treatment of VR

By means of the connectivity analysis of the TCM–target network, it was established that among the 56 genes involved in regulation by GXDSF, the number of genes with connectivity degrees 1, 2, and 3 are 20, 15, and 21, respectively (as shown in Fig. 7.13). This implies that in GXDSF, there are 21 VR-related genes that 3 Chinese herbs act on concurrently, 15 VR-related genes that at least two kinds of Chinese herbs act on concurrently, and 20 VR-related genes that only 1 kind of Chinese herb acts upon.

7.3.3.3 Discovery of the Potential Pathway of GXDSF in the Treatment of VR

The KEGG pathway enrichment analysis was implemented using GXDSF target protein overlapped with VR-related genes as the input. The results demonstrate that there are 75 VR-related pathways involved in the regulation through GXDSF. Table 7.3 provides the names, the corrected P-values, and the involved VR-related genes of each pathway. The results of pathway enrichment analysis reflect the characteristics of multi-target and multi-channel treatment of TCM compound prescriptions.

7.3.4 Verification and Summary

Through experimental research in the initial stage, the authors found that a variety of main active ingredients in Guanxin Danshen Formulation can combine with estrogen receptor to produce an estrogen like effect, and exhibit anti-inflammatory, antioxidant, anti-apoptotic [4], and neuroprotective effects [10] by regulating ERs-PI3K/Akt signaling pathway. Based on the results of pathway enrichment and its topological parameter—connectivity in the network, and combined with previous studies, we hand-picked ERs-PI3K/Akt signaling pathway from the above 75 pathways to verify the pharmacodynamic mechanism of action of ERs-PI3K/Akt signaling pathway in the Guanxin Danshen Formulation against MIRI-LVR.

7.3.4.1 Expression of ERs-PI3K/Akt Signaling Pathway-Related Proteins of Guanxin Danshen Formulation Against MirI-LVR Rat Myocardial Tissue

Western Blot results demonstrate that compared to the sham-operated group, the expression quantity of estrogen receptor α and β in the MIRI-LVR model group increased, but there was no significant difference. Simvastatin also had no significant effect on the expression of estrogen receptors. Upon being treated with Guanxin Danshen Formulation, the expression of ERα in myocardial tissue was not significantly affected either, however, the expression quantity of Erβ increased in acceptable doses. Correspondingly, with the increase of ERβ expression quantity, the phosphorylation level of PI3K/Akt in the downstream signaling pathway protein PI3K/Akt in myocardial tissue increased significantly. The results are shown in Fig. 7.14.

The effect of Guanxin Danshen Formulation on the distribution of ERβ/α-SMA in myocardial tissue of MIRI-LVR model rats was investigated by immunofluorescence double staining. The results demonstrate that the expression of ERβ in the MIRI-LVR model group did not significantly increase compared to the

Table 7.3 Potential Pathway of GXDSF in the Treatment of VR

Serial No.	Pathway	Corrected *P*-value	Related genes
1	AGE-RAGE signaling pathway in diabetic complications	5.72×10^{-55}	AKT1|BAX|BCL2|CASP3|CCL2|COL1A1|EDN1|EGR1|FN1|ICAM1|IL1A|IL1B|IL6|MAPK1|MAPK3|MMP2|NFKB1|NOS3|PRKCA|RELA|SERPINE1|SMAD3|STAT3|TGFB1|TNF|VCAM1|VEGFA
2	Fluid shear stress and atherosclerosis	2.82×10^{-33}	AKT1|BCL2|CCL2|EDN1|FOS|HMOX1|ICAM1|IFNG|IL1A|IL1B|MMP2|MMP9|NFKB1|NOS3|PLAT|RELA|SQSTM1|TNF|VCAM1|VEGFA
3	HIF-1 signaling pathway	1.27×10^{-31}	AKT1|BCL2|EDN1|EGFR|HMOX1|IFNG|IL6|MAPK1|MAPK3|NFKB1|NOS2|NOS3|PRKCA|RELA|SERPINE1|STAT3|TIMP1|VEGFA
4	TNF signaling pathway	1.03×10^{-28}	AKT1|CASP3|CCL2|CCL5|EDN1|FOS|ICAM1|IL1B|IL6|MAPK1|MAPK3|MMP9|NFKB1|PTGS2|RELA|TNF|VCAM1
5	IL-17 signaling pathway	1.12×10^{-20}	CASP3|CCL2|FOS|IFNG|IL1B|IL6|MAPK1|MAPK3|MMP9|NFKB1|PTGS2|RELA|TNF
6	Colorectal cancer	1.42×10^{-18}	AKT1|BAX|BCL2|CASP3|CASP9|FOS|MAPK1|MAPK3|MYC|SMAD3|TGFB1
7	PI3K-Akt signaling pathway	3.64×10^{-18}	AKT1|BCL2|BCL2L1|CASP9|COL1A1|EGFR|FN1|IL6|MAPK1|MAPK3|MYC|NFKB1|NOS3|PRKCA|RELA|VEGFA
8	Inflammatory bowel disease (IBD)	3.70×10^{-18}	IFNG|IL10|IL1A|IL1B|IL6|NFKB1|RELA|SMAD3|STAT3|TGFB1|TNF
9	EGFR tyrosine kinase inhibitor resistance	3.6×10^{-17}	AKT1|BAX|BCL2|BCL2L1|EGFR|IL6|MAPK1|MAPK3|PRKCA|STAT3|VEGFA
10	MAPK signaling pathway	1.46×10^{-16}	AKT1|CASP3|EGFR|FOS|IL1A|IL1B|MAPK1|MAPK3|MYC|NFKB1|PRKCA|RELA|TGFB1|TNF
11	Apoptosis	2.46×10^{-16}	AKT1|BAX|BCL2|BCL2L1|CASP3|CASP9|FOS|MAPK1|MAPK3|NFKB1|RELA|TNF
12	Prion diseases	2.56×10^{-16}	BAX|CCL5|EGR1|IL1A|IL1B|IL6|MAPK1|MAPK3|SOD1
13	Endocrine resistance	3.13×10^{-16}	AKT1|BAX|BCL2|EGFR|ESR1|ESR2|FOS|MAPK1|MAPK3|MMP2|MMP9
14	Th17 cell differentiation	1.23×10^{-15}	FOS|IFNG|IL1B|IL6|MAPK1|MAPK3|NFKB1|RELA|SMAD3|STAT3|TGFB1
15	NOD-like receptor signaling pathway	3.20×10^{-15}	ATG5|BCL2|BCL2L1|CCL2|CCL5|IL1B|IL6|MAPK1|MAPK3|NFKB1|RELA|TNF
16	Small cell lung cancer	1.05×10^{-14}	AKT1|BCL2|BCL2L1|CASP9|FN1|MYC|NFKB1|NOS2|PTGS2|RELA
17	FoxO signaling pathway	1.34×10^{-14}	AKT1|CAT|EGFR|IL10|IL6|MAPK1|MAPK3|SMAD3|SOD2|STAT3|TGFB1

(continued)

Table 7.3 (continued)

Serial No.	Pathway	Corrected *P*-value	Related genes
18	Apelin signaling pathway	2.22×10^{-14}	ACTA2|AKT1|EGR1|MAPK1|MAPK3|NOS2|NOS3|PLAT|PPARGC1A|SERPINE1|SMAD3
19	Estrogen signaling pathway	5.23×10^{-14}	AKT1|EGFR|ESR1|ESR2|FOS|MAPK1|MAPK3|MMP2|MMP9|NOS3
20	Non-alcoholic fatty liver disease (NAFLD)	5.26×10^{-14}	AKT1|BAX|CASP3|IL1A|IL1B|IL6|NFKB1|PPARA|RELA|TGFB1|TNF

sham-operated group, but the expression distribution of α-SMA in the myocardial infarction area and the infarction boundary area significantly increased. Compared to the model group, the expression distribution of α-SMA in the infarct zone and the infarct border zone of the simvastatin group decreased; the expression of ERβ in myocardial tissue in the border zone of infarction increased with the increase of dose in low, medium, and high dose groups of Guanxin Danshen Formulation. Concurrently, the expression of α-SMA in the infarct area and infarct border area decreased with the increase of dose. The results are demonstrated in Fig. 7.15.

The results advocate that the Guanxin Danshen Formulation can promote the expression of ERβ in myocardial tissue in acceptable doses, and in the interim, increase the phosphorylation of PI3K/Akt in its downstream signaling pathway. It indicates that the myocardial protective effect of Guanxin Danshen Formulation may be related to the selective activation of ERβ/PI3K/Akt signaling pathway.

7.3.4.2 Verification of the Pharmacodynamic Mechanism of Action of ERs-PI3K/Akt Signaling Pathway in Guanxin Danshen Formulation Against MIRI-LVR

Effect of Inhibiting ERβ on the Therapeutic Effect of Guanxin Danshen Prescription Against MIRI-LVR

The test results of myocardial three enzymes show that the levels of myocardial three enzymes do not change significantly after MIRI-LVR model rats are treated with PHTPP alone. Compared with the Guanxin Danshen Formulation treatment group, the LDH ($P < 0.001$) and CK-MB ($P < 0.05$) increased significantly in the +PHTPP Guanxin Danshen Formulation treatment group. The results are shown in Fig. 7.16.

The results of Masson staining demonstrate that there is no significant change in the area of myocardial fibrosis in MIRI-LVR model rats after being treated with PHTPP. Compared to the Guanxin Danshen Formulation treatment group, the area of myocardial fibrosis increased significantly in the +PHTPP Guanxin Danshen Formulation treatment group ($P < 0.01$). Western Blot testing of α-SMA expression level in myocardial tissue exhibits no significant change in the expression level of α-SMA in MIRI-LVR model rats treated with PHTPP. Compared to the Guanxin

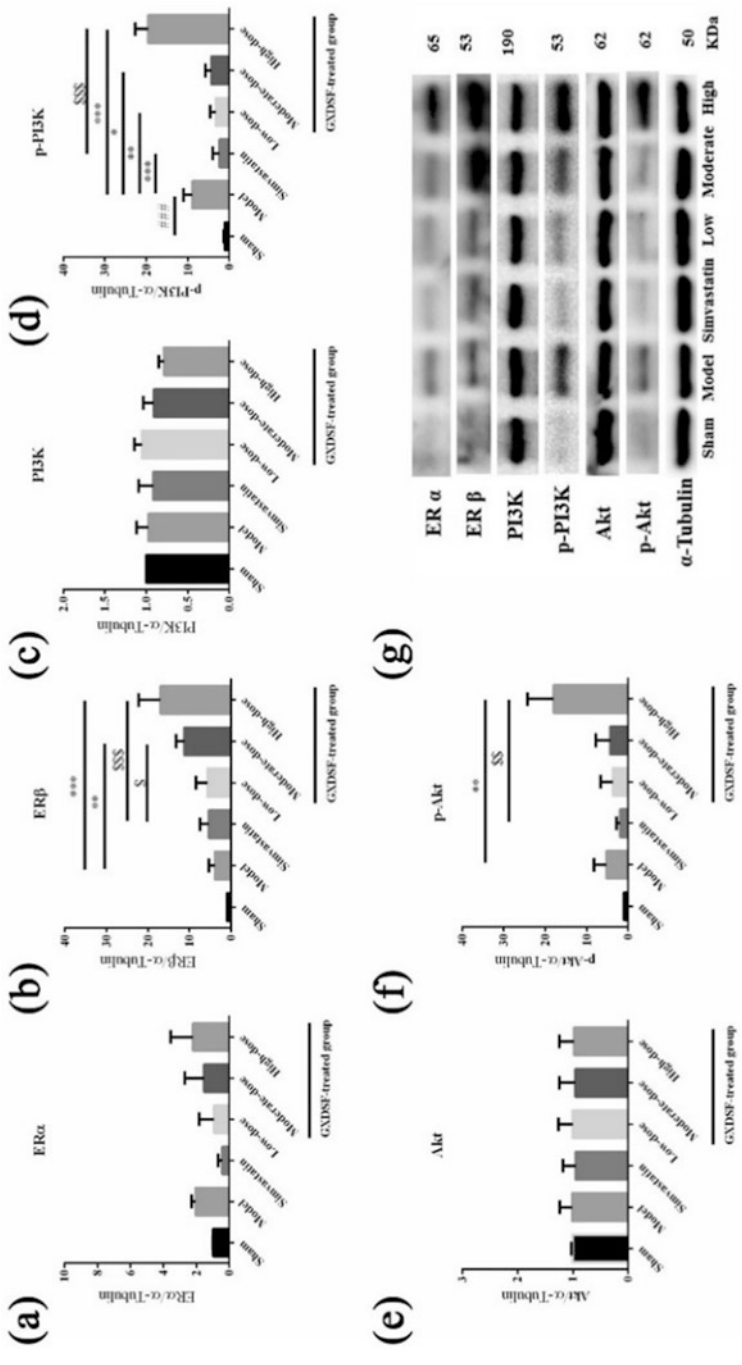

Fig. 7.14 Effect of Guanxin Danshen formulation on protein expression in estrogen receptor and its downstream signaling pathway

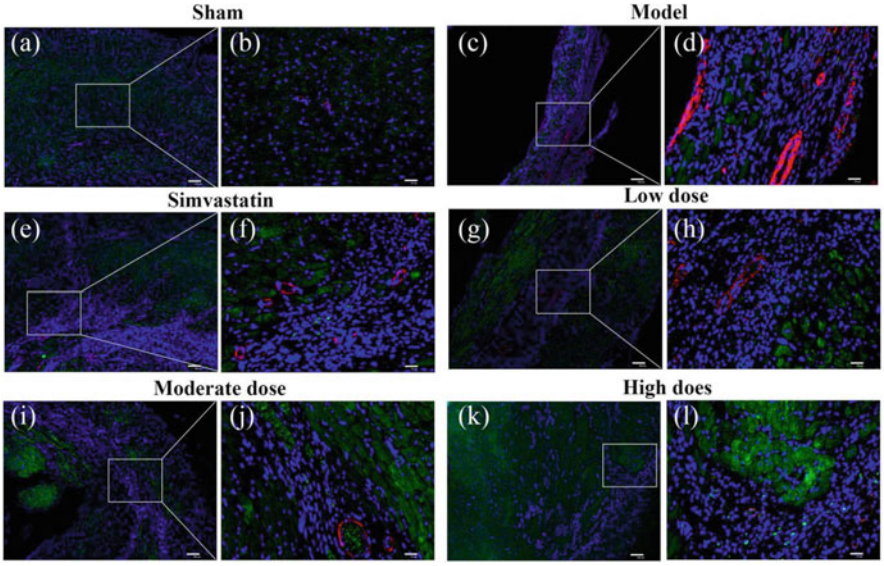

Fig. 7.15 Effect of Guanxin Danshen formulation on expression and distribution of ERβ/α-SMA in myocardial tissues (the bar value of (**a**, **c**, **e**, **g**, **i**, and **k**) is 100 μm, and that of (**b**, **d**, **f**, **h**, **j**, and **i**) is 25 μm)

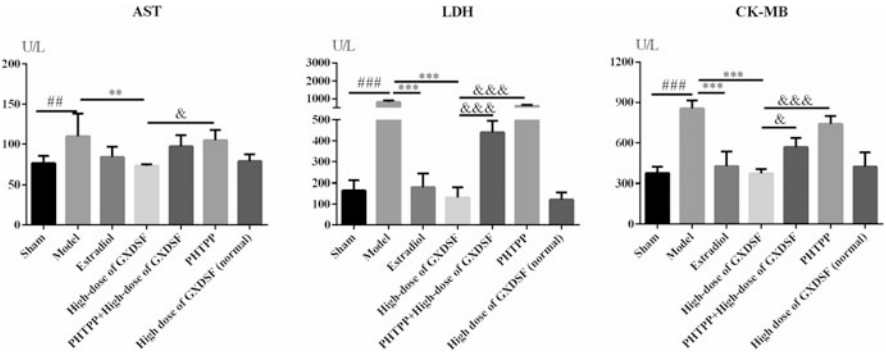

Fig. 7.16 Effect of ERβ inhibitor PHTPP on the expression of three enzymes in myocardium of Guanxin Danshen formulation

Danshen Formulation treatment group, the expression level of α-SMA increased significantly in the +PHTPP Guanxin Danshen Formulation treatment group ($P < 0.001$). The results are shown in Fig. 7.17.

The shown heart function test results of Hemodynamics (as shown in Fig. 7.18) and echocardiography (as shown in Fig. 7.19) indicate that there are no significant changes in the LVSP, +DP/DT, LVEF, and LVFS of MIRI-LVR model rats after being treated with PHTPP. Compared to the Guanxin Danshen Formulation treatment group, the LVSP ($P < 0.05$), +dp/dt ($P < 0.05$), LVEF ($P < 0.01$), and LVFS

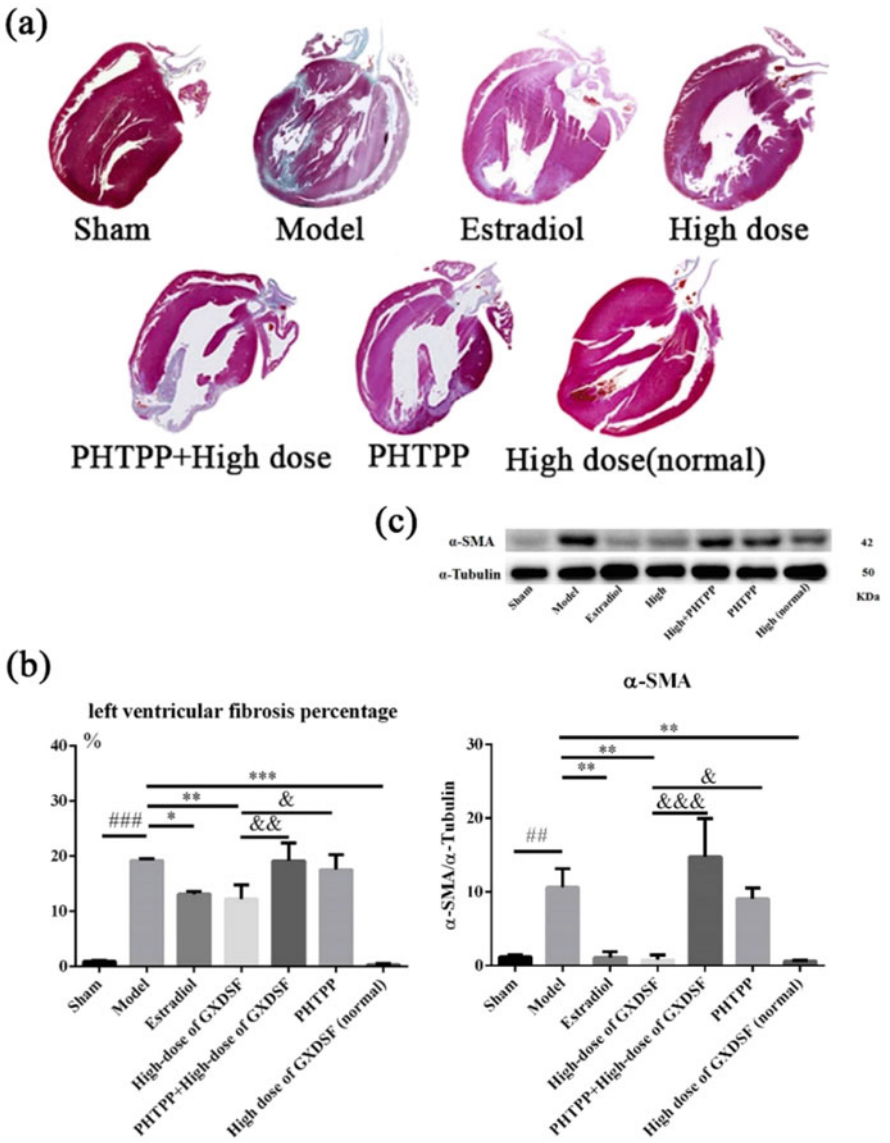

Fig. 7.17 Effect of ERβ Inhibitor PHTPP on reversing myocardial fibrosis of Guanxin Danshen formulation. (**a**) Results of Masson staining in myocardial tissue sections; (**b**) Statistical results of fibrotic area in Masson staining sections; (**c**) Western blot detection of α-SMA expression quantity results in myocardial tissue

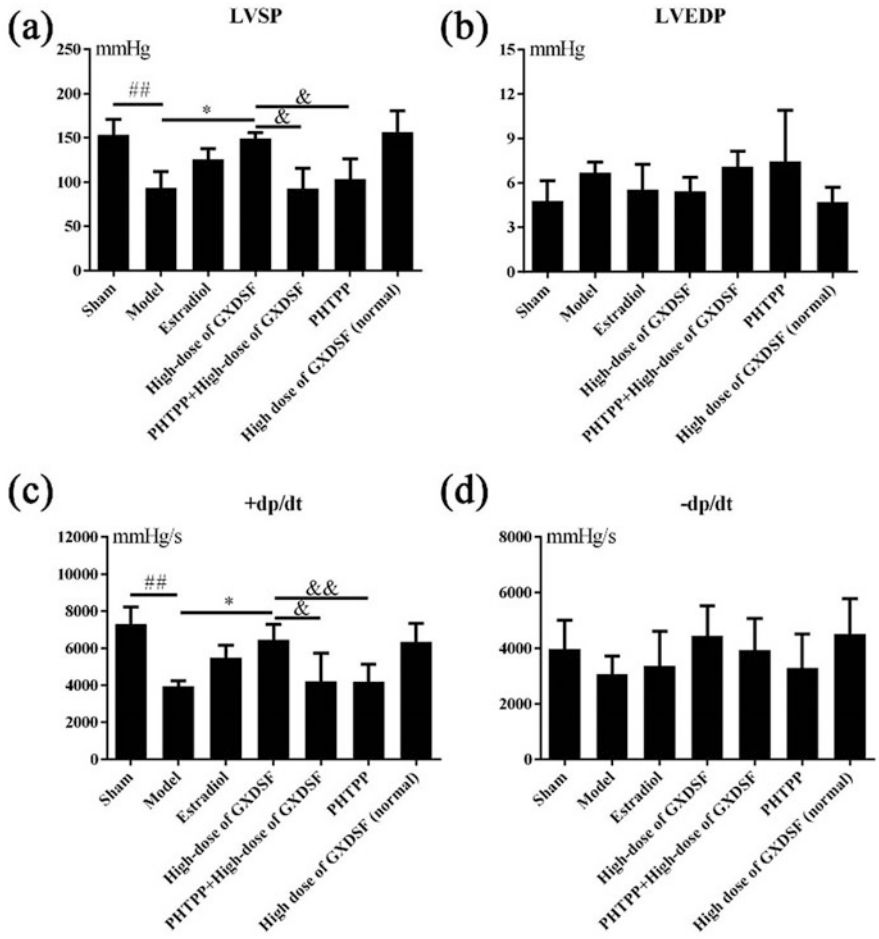

Fig. 7.18 Effect of Erβ inhibitor PHTPP on Guanxin Danshen formulation in improving the hemodynamic indexes

($P < 0.05$) decreased significantly in the +PHTPP Guanxin Danshen formulation treatment group. There are significant differences when comparing LVEF ($P < 0.05$) and LVFS ($P < 0.05$) between 17β-estradiol group and Guanxin Danshen formulation group.

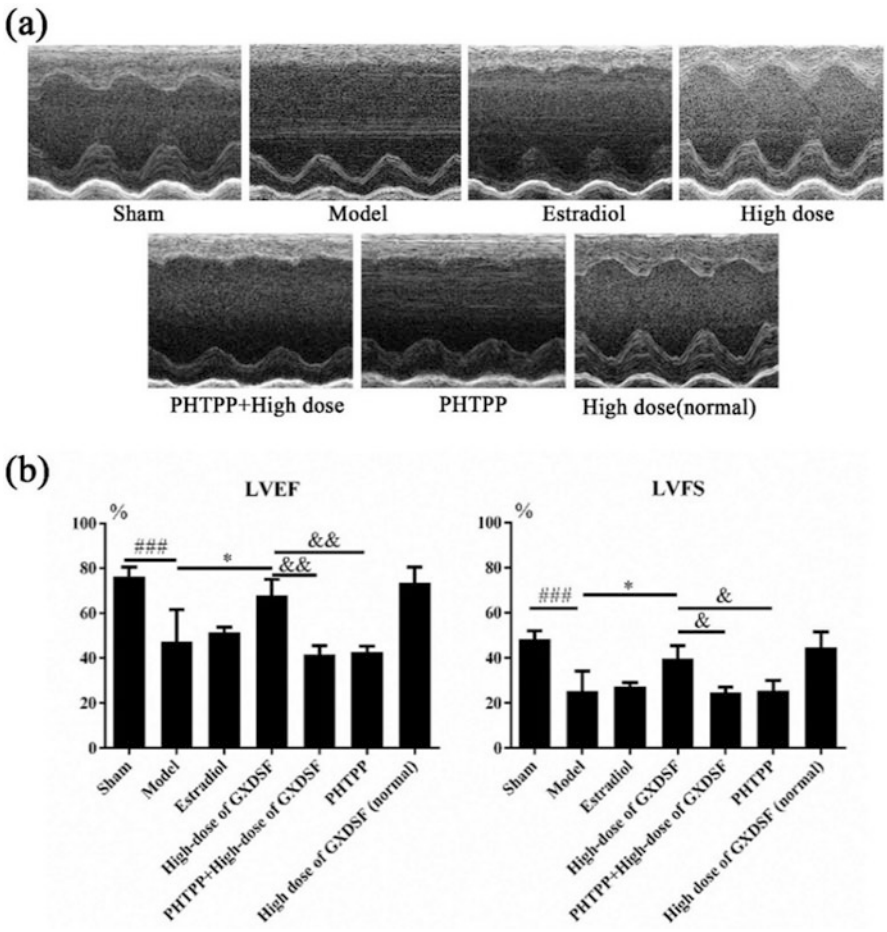

Fig. 7.19 Effect of Erβ inhibitor PHTPP on Guanxin Danshen formulation in improving the echocardiographic indexes

Effects of Inhibiting ERβ on the Protein and Signaling Pathway that Guanxin Danshen Formulation Acts Upon

The results of expression of estrogen receptor β and its downstream signaling pathway PI3K/Akt detected by Western Blot indicate that, compared to the sham-operated group, Guanxin Danshen Formulation has no significant effect on the expression of estrogen receptor β and its downstream signaling pathway PI3K/Akt in normal rat myocardial tissue. Upon PHTPP treatment, compared to the Guanxin Danshen Formulation treatment group, the expression of estrogen receptor β in the +PHTPP group of Guanxin Danshen Formulation significantly decreased ($P < 0.001$), and its phosphorylation level of PI3K/Akt in downstream signaling pathway also significantly decreased ($P < 0.001$). The results are shown in Fig. 7.20.

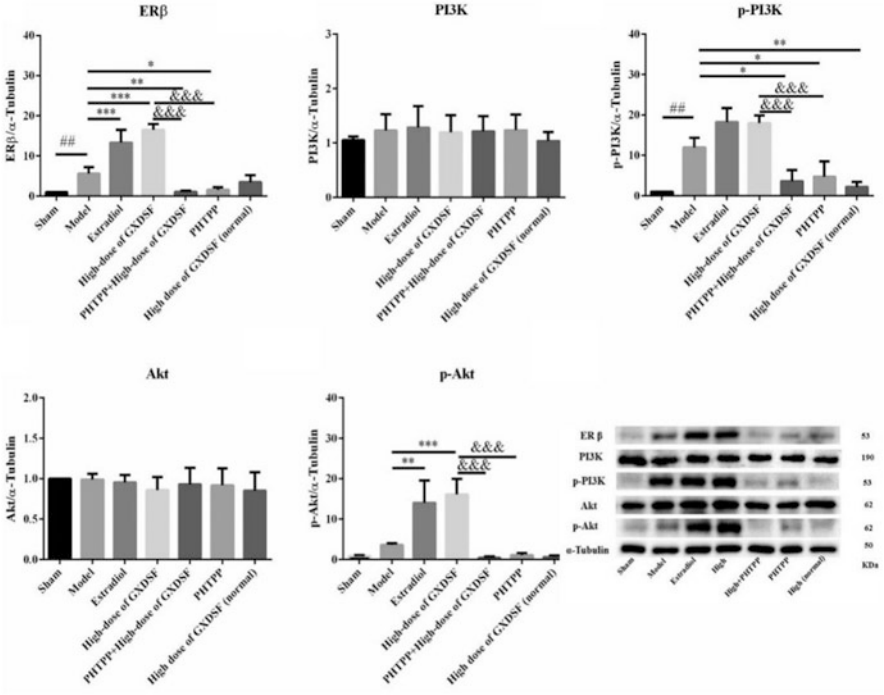

Fig. 7.20 Effect of ERβ Inhibitor PHTPP on the protein and signaling pathway that Guanxin Danshen formulation acts upon

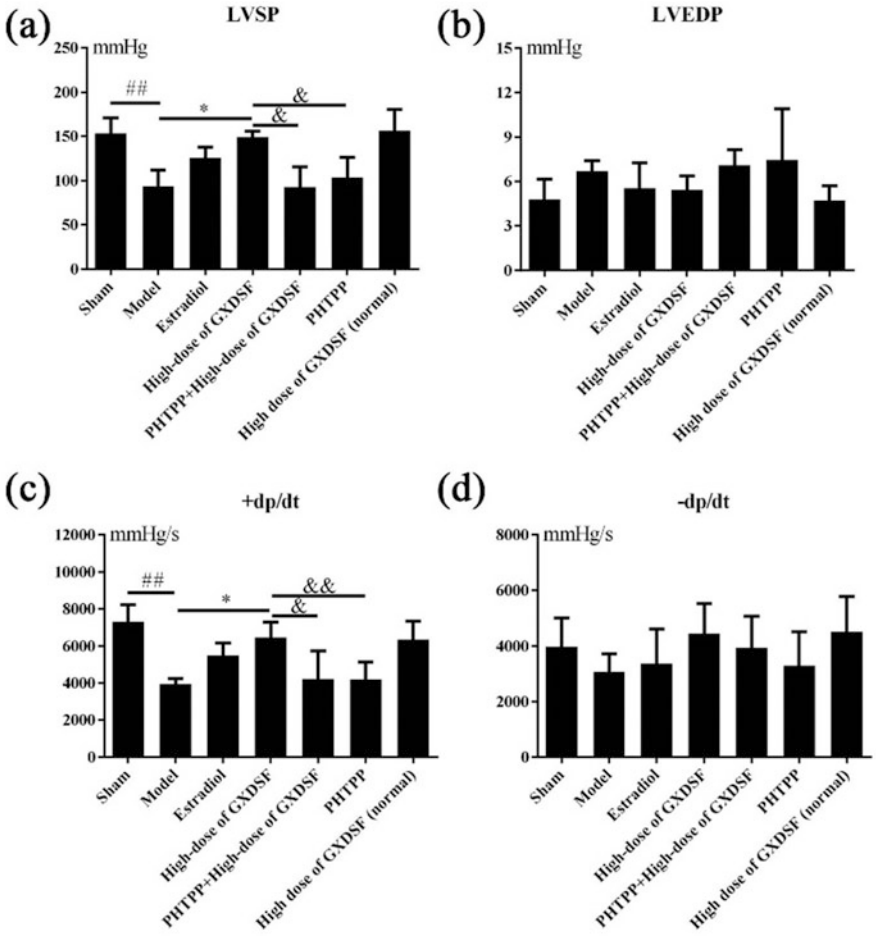

The effects of PHTPP on the expression distribution of ERβ/α-SMA tested by immunofluorescence double staining indicate that, after treatment with PHTPP, the expression of estrogen receptor β in the infarct area and the infarct border area of MIRI-LVR rats significantly decreased, and the expression of α-SMA in the infarct area and the infarct border area significantly increased. Compared to the Guanxin Danshen Formulation treatment group, the expression of ERβ in the myocardial tissue of infarction area and infarct boundary area was significantly inhibited in the +PHTPP Guanxin Danshen Formulation treatment group, and in the interim, a large number of expression and distribution of α-SMA can be observed. The results are shown in Fig. 7.21.

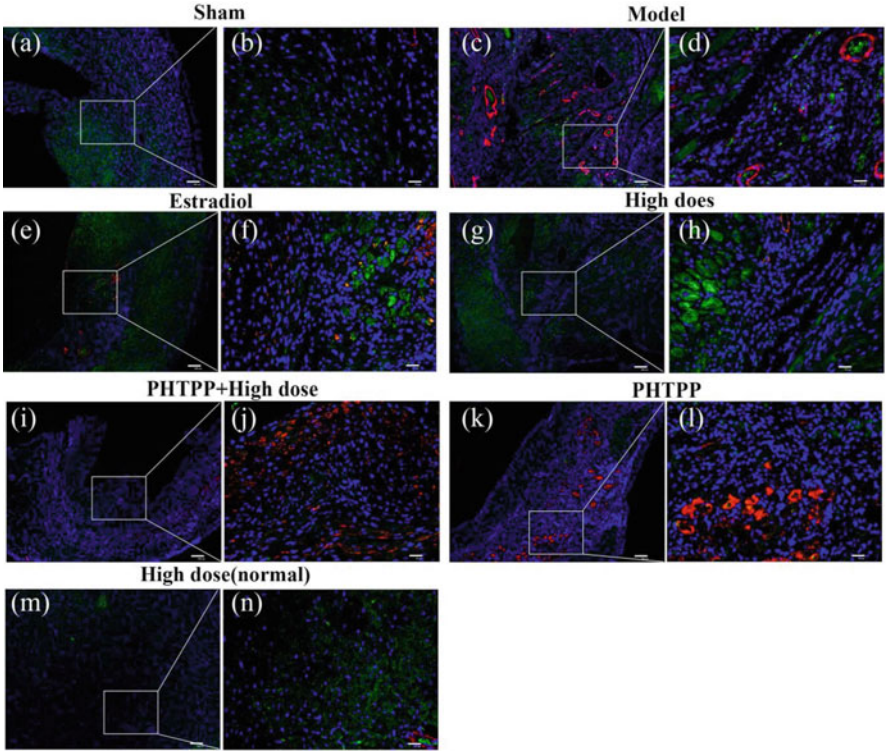

Fig. 7.21 Effect of ERβ Inhibitor PHTPP on the Expression Distribution of ERβ/α-SMA (the bar value of (**a**, **c**, **e**, **g**, **i**, **k**, and **m**) is 100 μm, and that of (**b**, **d**, **f**, **h**, **j**, **i**, and **n**) is 25 μm)

7.3.4.3 Summary

This section cites the classic and famous GXDSF Formulation as an example to exhaustively introduce the experimental reasoning and measures of investigating the efficacy mechanism of Chinese herbal compound prescriptions based on the network pharmacology method, with a view to provide research reasoning and reference for the investigation of the mechanism of action of TCM/TCM compound prescriptions. Contingent on ETCM, TCM-MESH, CTD database, and Cytoscape analysis software, this section constructs a TCM–target–disease network of GXDSF against MIRI-LVR based on the network pharmacology method. Using network analysis, we identified 75 signaling pathways, which collectively constitute the pharmacodynamic network of GXDSF. The pathway enrichment results and topological parameters—connectivity in the network, were integrated and combined with the basis of previous research, and we hand-picked the ERs-PI3K/Akt signaling pathway from the above 75 pathways to verify the pharmacodynamic mechanism of GXDSF against MIRI-LVR through experiments. The verification results demonstrated that Guanxin Danshen Formulation could significantly promote the expression of ERβ

and its downstream signaling pathway protein PI3K/Akt in the myocardial tissue of MIRI-LVR model rats in acceptable doses. PHTPP, a specific inhibitor of ERβ in rats, was rendered to verify the role of ERβ in the myocardial protection capabilities of Guanxin Danshen Formulation. The results demonstrated that PHTPP could significantly aggravate the improvement of three myocardial enzymes and the improvement of cardiac structure and function by Guanxin Danshen Formulation. It indicates that the myocardial protective effect of Guanxin Danshen Formulation is closely related to the activation of ERβ/PI3K/Akt signaling pathway. In summation, we discovered the pharmacodynamic mechanism network of GXDSF by employing the analysis method of network pharmacology, and verified the significant function of ERβ/PI3K/Akt signaling pathway in the pharmacodynamics of GXDSF by means of animal model experiments [11]. The results of network analysis are highly consistent with the experimental results, which indicate that network pharmacology is an effective means to investigate the pharmacodynamic mechanism of TCM/TCM compound prescriptions.

7.4 Explanation of the Interaction Between TCM and Western Medicine: Combined Use of Chinese and Western Medicines Enhances Efficacy and Reduces Toxicity

Ischemic stroke is a global health problem, accounting for more than 77% of all strokes, and is the leading cause of disability and the second leading cause of mortality globally, with a growing mortality rate [12]. Although great progress has been made in the pathophysiological mechanism of ischemic stroke in China and overseas in recent years, there are still very limited clinical drugs for the treatment of ischemic stroke. So far, the only drug approved for the treatment of acute ischemic stroke is recombinant tissue plasminogen activator (rt-PA). However, the application of rt-PA is limited due to the short treatment time window (3 h) and potential side effects (intracranial hemorrhage) [13]. Thrombolytic therapy is only suitable for acute stage of ischemic stroke. At present, aspirin, which is commonly used in clinical treatment and prevention of cerebrovascular disease, is only effective for patients with mild stroke, and the therapeutic effect is not satisfactory. The CHANCE study conducted by Professor Wang Yong-jun found that, for patients with mild stroke and TIA within 24 h of onset, giving them a combination of aspirin and clopidogrel for 21 consecutive days (grade B evidence, grade IIb recommendation) was effective in reducing stroke recurrence within 90 days, confirming that the combined use of aspirin and clopidogrel is more effective than using aspirin alone. Although the efficacy of combined antiplatelet therapy is better than that of aspirin alone, combined antiplatelet therapy also has limitations related to the appropriate population, bleeding risk, and gastrointestinal mucosal injury. As existing clinical drugs have not yet met the clinical needs, there is an urgent need for new treatment

strategies for acute ischemic stroke. The activating blood and removing blood stasis agent, clearing heat and resuscitating agent, replenishing qi and promoting blood circulation agent among Chinese patent medicines, such as Panax notoginseng, Salvia miltiorrhiza, Ligusticum chuanxiong, and Ginkgo biloba preparations with clinically definite curative effects, have received increasing attention recently due to their unique effects. Therefore, finding more effective treatment methods and drugs for stroke has become a key topic of discussion in the field of pharmaceutical research.

Panax notoginseng is a traditional and precious traditional Chinese medicine in China, enjoying the reputation of "Jinbuchang," "Magic medicine from Nan'guo," "King of Ginseng," and "surgical elixir." [14] The *Supplement to Compendium of Materia Medica* records that: "Ginseng supplements qi first, panax notoginseng supplements blood first, having the same taste but different functions, thus it is called panax notoginseng, the most precious of Traditional Chinese medicine." [15] Panax notoginseng is the root of the perennial herbaceous plant Araliaceae. It is sweet and slightly bitter in taste, wet in nature, and attributive to liver, and stomach channels. Raw Panax notoginseng reduces blood stasis and stops bleeding, and can be used for hemoptysis, vomiting blood, bruises, swelling and pain, and traumatic bleeding; cooked Panax notoginseng replenishes blood and promotes blood circulation, and is used for blood loss and anemia [16]. By constructing an integrated pharmacology based on the integration of network pharmacology, genomics, systematic pharmacology, and other technologies, this research group analyzed the multi-level research technology of the mechanism of action of panax notoginseng, promoted the clinical positioning and re-evaluation of original new drugs, and clarified panax notoginseng's pharmacodynamic material basis. Xuesaitong is developed from the effective active ingredients in Panax notoginseng. In vivo and in vitro studies in China and overseas have proved that it has definite cardioprotective effect, such as inhibiting platelet aggregation, reducing blood viscosity, antithrombotic effect, improving microcirculation, inhibiting inflammatory reaction, activating estrogen receptor in playing an anti-apoptosis role, etc. [17] The Xuesaitong Soft Capsule has the effect of promoting blood circulation and removing blood stasis, dredging blood vessels, and activating collaterals. It is mainly used during the recovery period of the meridian in stroke for the blood stasis and closed channels and collaterals syndrome. Symptoms include hemiplegia, askew tongue, hard tongue, tough pronunciation of words, or inability to speak. Symptoms include hemiplegic paralysis, hemiparalysis, deviation of the eye and mouth, stiff tongue. In vitro and in vivo studies in China and overseas have proved that it has antioxidative stress and anti-inflammatory effects, and has definite neuroprotective effects.

According to the big data analysis of clinical data, at present, the traditional Chinese patent medicines for the treatment of acute ischemic stroke are mainly drugs for promoting blood circulation and removing blood stasis. To achieve symptomatic treatment, it is supplemented by Huatan Xingnao Kaiqiao medicine, while the use of Western medicine is recommended according to the guidelines for diagnosis and treatment of acute ischemic stroke. The combination of Chinese patent medicine and

Western medicine is mostly blood activating and stasis removing drugs + antiplatelet drugs [18]. Clinical findings show that the efficacy of using aspirin alone and the combined use of aspirin and clopidogrel could not meet the clinical needs. Moreover, due to the side effects of long-term use of aspirin, such as gastrointestinal mucosal injury and the risk of bleeding, antiplatelet drugs are not used alone in clinical use. Although it was found that the effect of combined use of Chinese patent medicine and antiplatelet drug is better than that of single use, there is a lack of quantitative data support for combined applications, and its action link, efficacy target, use dosage, multi-target synergistic effect enhancement, and toxicity reduction mechanism are as yet unclear. Therefore, we chose to adopt MCAO/R model rats.

7.4.1 Data Acquisition and Processing

The research idea and process are shown in Fig. 7.22.

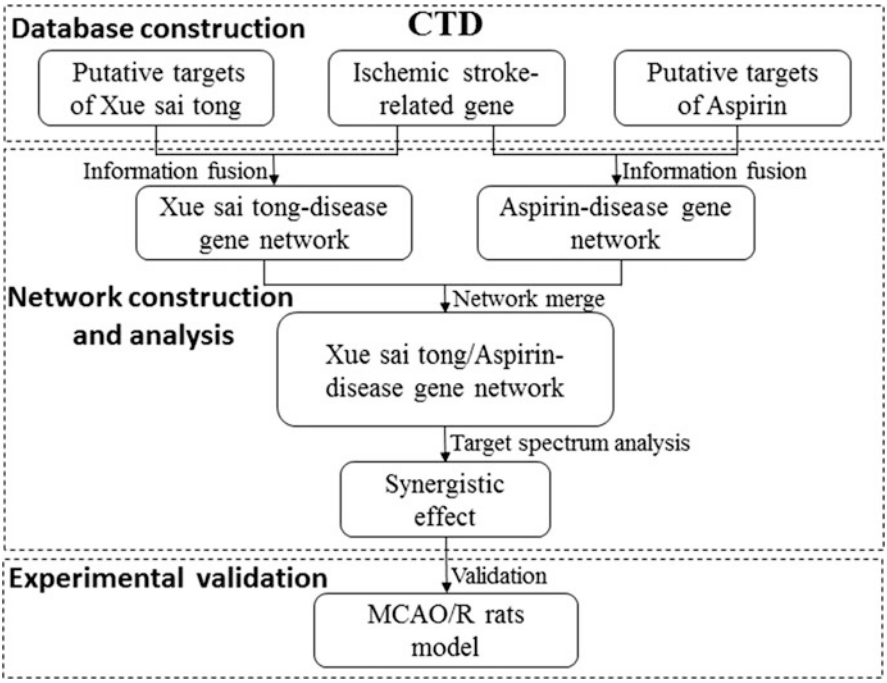

Fig. 7.22 Research ideas and processes

7.4.1.1 Selection of Target Components

Based on references and our previous experimental results, five main effective ingredients—notoginsenoside R1, ginsenoside Rg1, ginsenoside Rb1, ginsenoside Rd, and ginsenoside Re (as shown in Table 7.4) were selected as the representative ingredients of Xuesaitong for carrying out the subsequent study.

7.4.1.2 Collection of Chemical Composition Targets

"Chemicals" was selected under the Keyword Search option of the CTD database, the English name of each chemical component was entered in the search box, and the target data of each chemical component collected. The corresponding relationship between each chemical component and its targets was saved in the form of a two-dimensional list.

7.4.1.3 Gene Collection of Ischemic Stroke-Related Diseases

"Diseases" was selected under the Keyword Search option of the CTD database, and "Cerebral infarction/Brain infarction" was entered in the search box to collect the gene data related to ischemic stroke. The corresponding relationship between each gene and ischemic stroke was saved in the form of a two-dimensional list.

Table 7.4 Main effective ingredients of Xuesaitong

Serial No.	Compound	Chinese name	CAS	Molecular formula	Molecular weight
1	Notoginsenoside R1	三七皂苷 R1	80418-24-2	$C_{47}H_{80}O_{18}$	933.139
2	Ginsenoside Rg1	人参皂苷 Rg1	22427-39-0	$C_{42}H_{72}O_{14}$	801.024
3	Ginsenoside Rb1	人参皂苷 Rb1	41753-43-9	$C_{54}H_{92}O_{23}$	1109.307
4	Ginsenoside Rd	人参皂苷 Rd	52705-93-8	C48H82O18	947.15
5	Ginsenoside Re	人参皂苷 Re	52286-59-6	C48H82O18	947.15

7.4.2 Network Construction and Visualization

7.4.2.1 Network Construction and Visualization

The "component–target" list and "disease–gene" list obtained from the data source were entered into the Cytoscape 3.5.0 network analysis and visualization software. The merge function under the "Tools" in the menu bar was used to superimpose the network, and construct "Xuesaitong-ischemic stroke target network," "Aspirin-ischemic stroke target network," and "Xuesaitong and Aspirin-Ischemic Stroke target network." Based on the drug–target network, the target profiles and the interaction between Xuesaitong and Aspirin were analyzed.

7.4.2.2 Analysis Index and Algorithm

The NetworkAnalyzer function under the "Tools" option in the Cytoscape 3.5.0 menu bar was used to analyze the topological attributes (connectivity) of each node in the network.

7.4.3 Network Analysis and Prediction

7.4.3.1 Target Network of Xuesaitong in the Treatment of Ischemic Stroke

Figure 7.23 shows the target network of Xuesaitong in the treatment of ischemic stroke. Notoginsenoside R1, Ginsenoside Rg1, ginsenoside Rb1, ginsenoside Rd, and ginsenoside Re regulate ischemic stroke by regulating 29, 18, 8, 9, and 23 genes related to ischemic stroke, respectively. There is a certain degree of crossover between the genes related to ischemic stroke regulated by each component. At the same time, each component has its specific regulatory target, reflecting the multi-component and multi-target characteristics of TCM. The genes with connectivity greater than 3 in the network are CASP3, CAT, TNF, BAX, BCL2, MAPK3, IL6, and MAPK1. These genes may be the key targets of Xuesaitong in the treatment of ischemic stroke.

7.4.3.2 Target Network of Aspirin in the Treatment of Ischemic Stroke

In treating ischemic stroke, aspirin regulates 62 genes related to ischemic stroke (as shown in Fig. 7.24). CASP3, CAT, TNF, BAX, BCL2, MAPK3, IL6, and MAPK1, which are regulated by Xuesaitong, are all reflected in the aspirin-ischemic stroke-related gene network, which further demonstrates the important role of these genes in the treatment process of ischemic stroke.

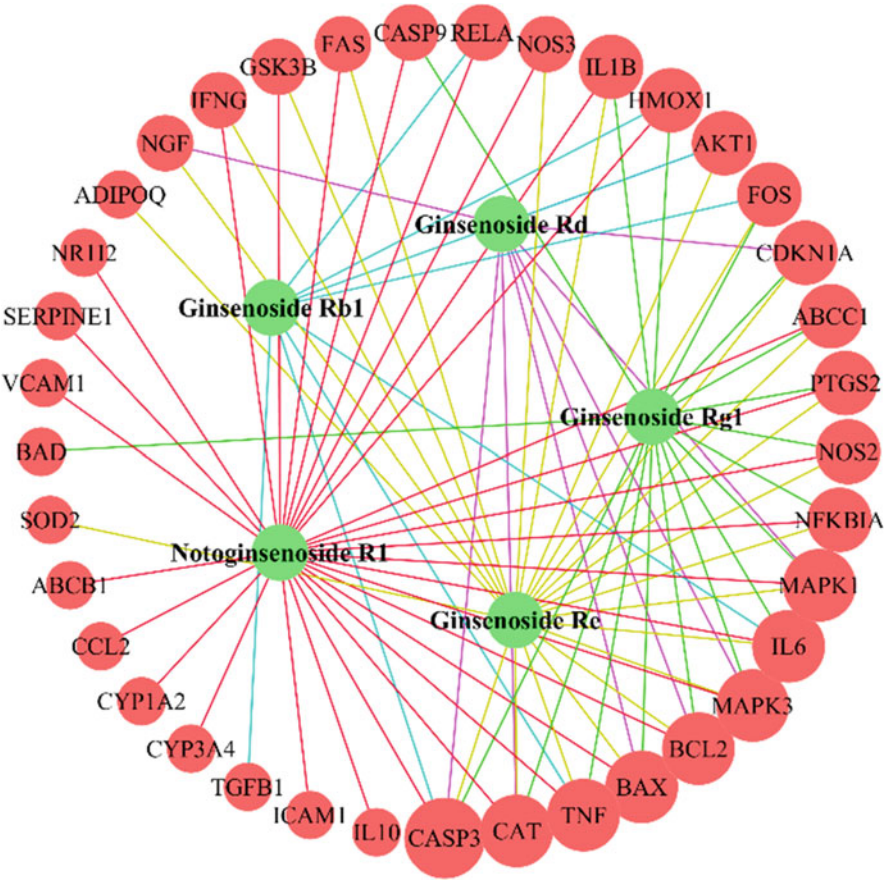

Fig. 7.23 Xuesaitong-ischemic stroke-related gene network. The green and red round nodes represent the main components of Xuesaitong and genes related to ischemic stroke, respectively

7.4.3.3 The Combined Use of Xuesaitong and Aspirin Enhances the Effect of Aspirin in Treating Ischemic Stroke

Figure 7.25 shows the molecular target network of combined use of aspirin and Xuesaitong. There is a high degree of overlap between aspirin and ischemic stroke-related genes regulated by Xuesaitong. Among the 37 genes regulated by Xuesaitong, 31 genes are overlapped with those regulated by aspirin, suggesting that the combined use of Xuesaitong and aspirin may have the potential to enhance the effect of aspirin in the treatment of ischemic stroke (as shown in Fig. 7.26). Compared with using aspirin alone, ischemic stroke-related genes regulated by the combined use of aspirin and Xuesaitong increased by 6 genes (CYP3A4, NRI12, NGF, CYP1A2, SERP1NE1, and ADIPOQ). However, the specific role of these genes in the combined use of aspirin and Xuesaitong still needs further research.

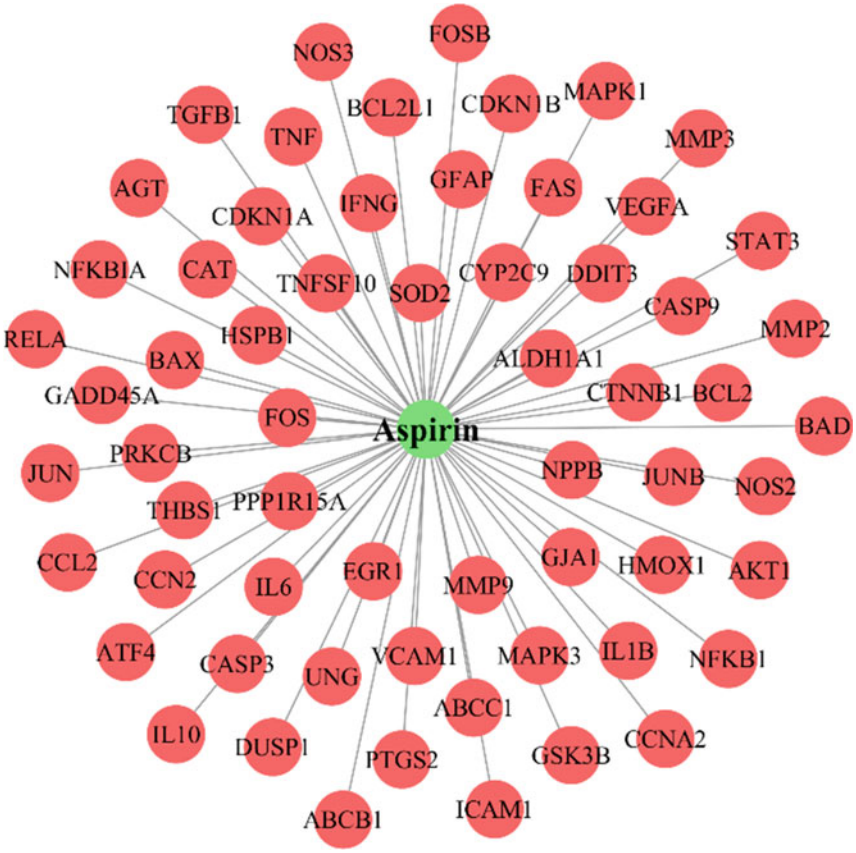

Fig. 7.24 Aspirin-ischemic stroke-related gene network. Green and red round nodes represent aspirin and ischemic stroke-related genes, respectively

7.4.4 Verification and Summary

7.4.4.1 Clinical Therapeutic Effect

A total of 120 patients with cerebral infarction treated from August 2015 to October 2017 were taken as research subjects and randomly divided into the treatment group and the control group with 60 cases each [19]. The treatment group was treated with the combined use of panax notoginseng saponins and aspirin, while the control group was treated with aspirin only. The therapeutic effect, platelet aggregation rate, recurrence rate, and complication rate of the two groups were compared. The total effective rate of 86.67% (52/60) in the treatment group was significantly higher than that of 71.67% (43/60) in the control group ($P < 0.05$). After treatment, the NIHSS score of the treatment group was significantly lower than that of the control group, the platelet aggregation rate was significantly lower than that of the control group,

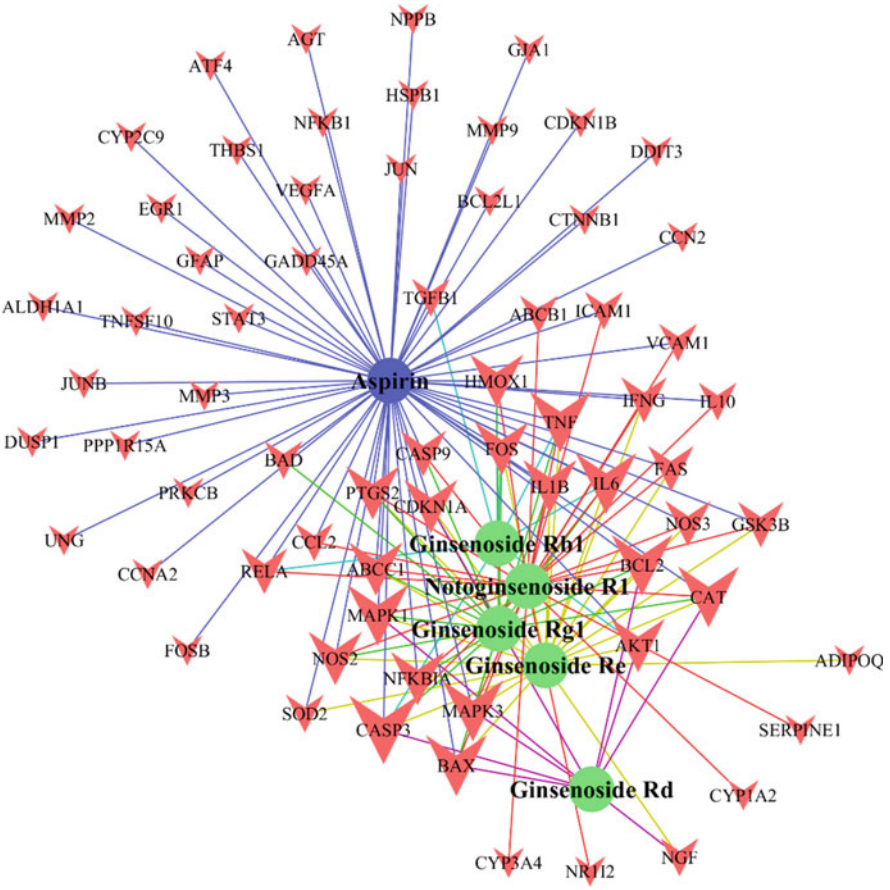

Fig. 7.25 Aspirin and Xuesaitong-ischemic stroke-related gene network. The green round nodes represent the main components of Xuesaitong, and the blue round nodes represent aspirin; the red V-shaped nodes represent genes associated with ischemic stroke. The blue, red, purple, yellow, green, and blue edges connect to the ischemic stroke-related genes associated with aspirin, notoginsenoside R1, ginsenoside Rd, ginsenoside Re, ginsenoside Rg1, and ginsenoside Rb1, respectively

the recurrence rate was significantly lower than that of the control group, and the incidence of complications was also significantly lower than that of the control group ($P < 0.05$). The combined use of panax notoginseng saponins and aspirin can achieve a certain preventive effect, which is safe and has a remarkable therapeutic effect on cerebral infarction.

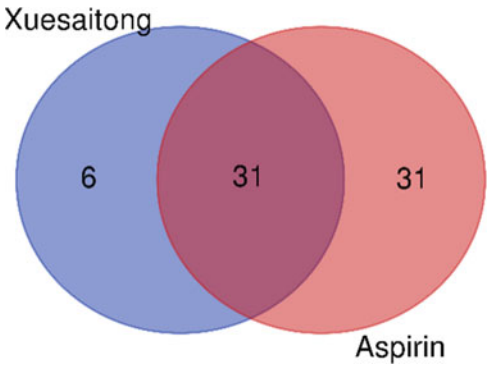

Fig. 7.26 Venn diagram—aspirin vs Xuesaitong (genes associated with ischemic stroke)

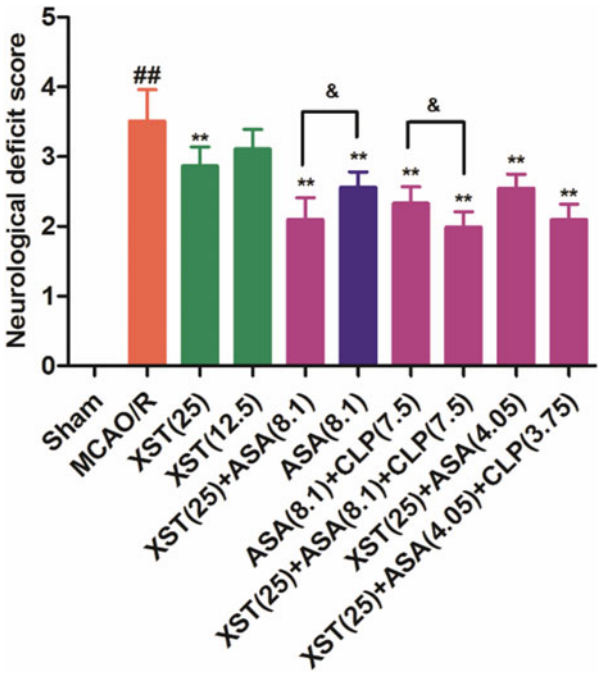

Fig. 7.27 Combined use of Xuesaitong and antiplatelet drugs significantly reduces the neurological deficit score of MCAO/R model rats. Note: ##, $P < 0.01$ vs sham-operated group; *, $P < 0.05$ vs MCAO/R Model group; △, $P < 0.05$ vs ASA group; &, $P < 0.05$ vs ASA+CLP group

7.4.4.2 Combined Use of Xuesaitong and Antiplatelet Drugs can Significantly Reduce the Neurological Deficit Score of MCAO/R Model Rats

As shown in Fig. 7.27, compared with the sham-operated group, the neurological deficit score of rats in the MCAO/R model group is increased significantly ($P < 0.05$); compared with the MCAO/R model group, Xuesaitong, aspirin, combined use of Xuesaitong and aspirin, combined use of clopidogrel and aspirin, combined use of Xuesaitong, aspirin, and clopidogrel, all significantly reduced the neurological

deficit score of rats ($P < 0.05$). Compared with aspirin (8.1 mg/kg) group, the combined use of Xuesaitong (25 mg/kg) and aspirin (8.1 mg/kg) significantly reduces neurological deficit score of rats ($P < 0.05$). Compared with the group using aspirin (8.1 mg/kg) and clopidogrel (7.5 mg/kg), the neurological deficit score of rats with the combined use of Xuesaitong (25 mg/kg), aspirin (8.1 mg/kg), and clopidogrel (7.5 mg/kg) is significantly decreased ($P < 0.05$).

7.4.4.3 Combined Use of Xuesaitong and Antiplatelet Drugs Significantly Reduces the Cerebral Infarction Volume in MCAO/R Model Rats

As shown in Fig. 7.28, compared with the sham-operated group, the cerebral infarction volume of rats in the MCAO/R model group is significantly increased ($P < 0.05$); compared with the MCAO/R model group, Xuesaitong, aspirin, combined use of Xuesaitong and aspirin, combined use of clopidogrel and aspirin, and combined use of Xuesaitong, aspirin, and clopidogrel, all significantly reduce the cerebral infarction volume ($P < 0.05$). Compared with the aspirin (8.1 mg/kg) group, the combined use of Xuesaitong (25 mg/kg) and aspirin (8.1 mg/kg) significantly reduces the cerebral infarction volume ($P < 0.05$). Compared with the group using aspirin (8.1 mg/kg) and clopidogrel (7.5 mg/kg), the cerebral infarction volume of rats with the combined use of Xuesaitong (25 mg/kg), aspirin (8.1 mg/kg), and clopidogrel (7.5 mg/kg) is significantly decreased ($P < 0.05$).

7.4.4.4 Combined Use of Xuesaitong and Antiplatelet Drugs Improves the Inhibitory Effect of Aspirin or Penicillin-Streptomycin on Platelets

As shown in Fig. 7.29, compared with the sham-operated group, the maximum platelet aggregation rate of the MCAO/R model group is significantly increased. Compared with the MCAO/R model group, use of aspirin, or combined use of clopidogrel and aspirin significantly reduces the maximum platelet aggregation rate. Combined use of Xuesaitong and aspirin, and combined use of Xuesaitong, aspirin, and clopidogrel significantly improve the inhibition of aspirin on platelets.

7.4.4.5 Xuesaitong Significantly Reduces Aspirin-Induced Gastric Mucosal Damage in Rats

As shown in Fig. 7.30, compared with the control group, gastric mucosal epithelial cells of rats are necrotic and inflammatory cells are infiltrated in the aspirin group. Compared with the aspirin group, Xuesaitong significantly reduces gastric mucosal epithelial cell necrosis and inflammatory cell infiltration induced by aspirin. Using Xuesaitong alone has no significant effect on the gastric mucosa of rats.

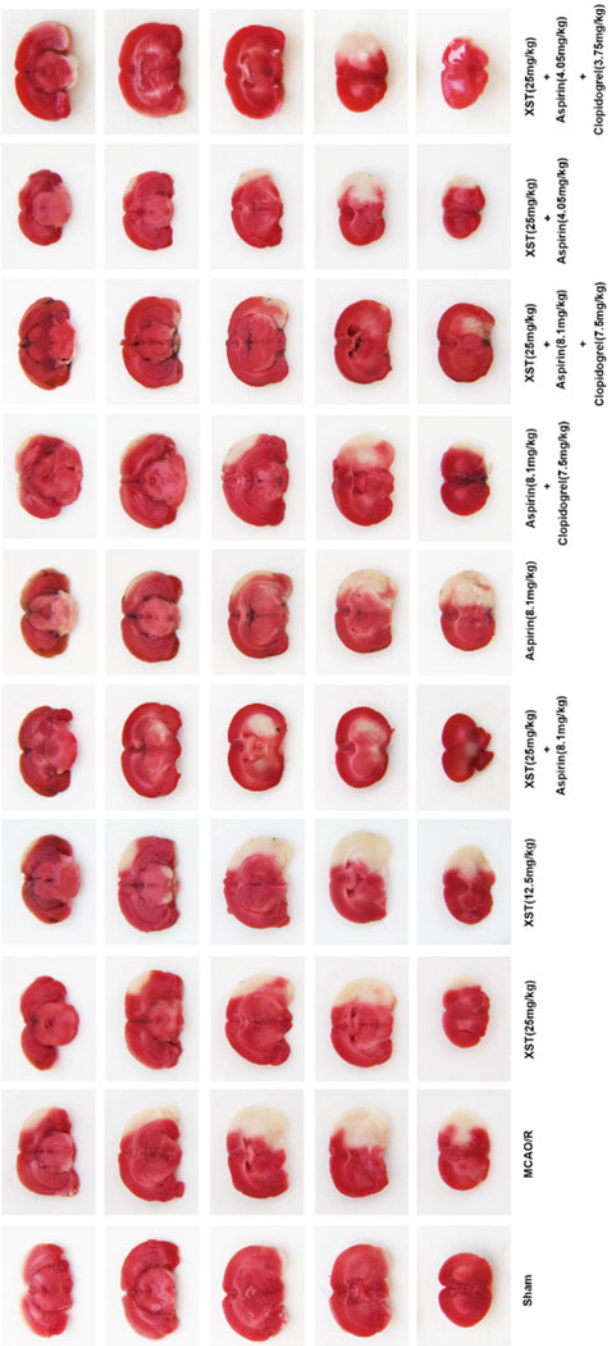

Fig. 7.28 Combined use of Xuesaitong and antiplatelet drugs significantly reduces the cerebral infarction volume in MCAO/R model rats. Note: ##, $P < 0.01$ vs sham-operated group *, $P < 0.05$ vs MCAO/R Model group; △, $P < 0.05$ vs ASA group; &, $P < 0.05$ vs ASA+CLP group

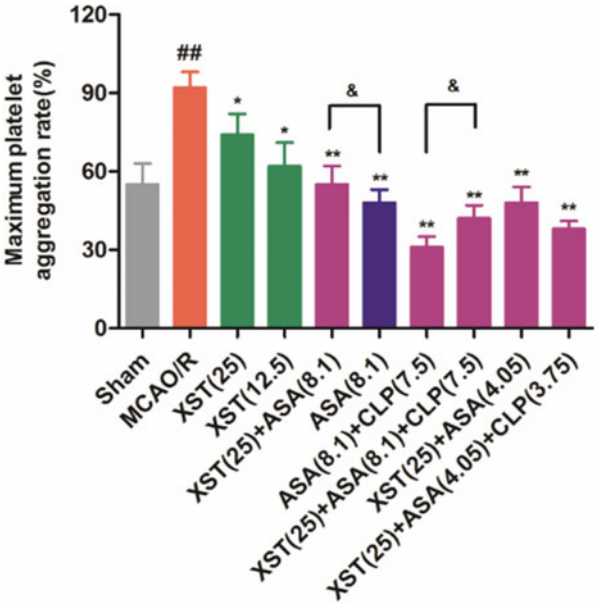

Fig. 7.29 Combined use of Xuesaitong and antiplatelet drugs improves the inhibitory effect of aspirin or penicillin-streptomycin on platelets. Note: ##, $P < 0.01$ vs sham-operated group; *, $P < 0.05$ vs MCAO/R Model group; **, $P < 0.01$ vs MCAO/R Model group; △, $P < 0.05$ vs ASA group; &, $P < 0.05$ vs ASA+CLP group

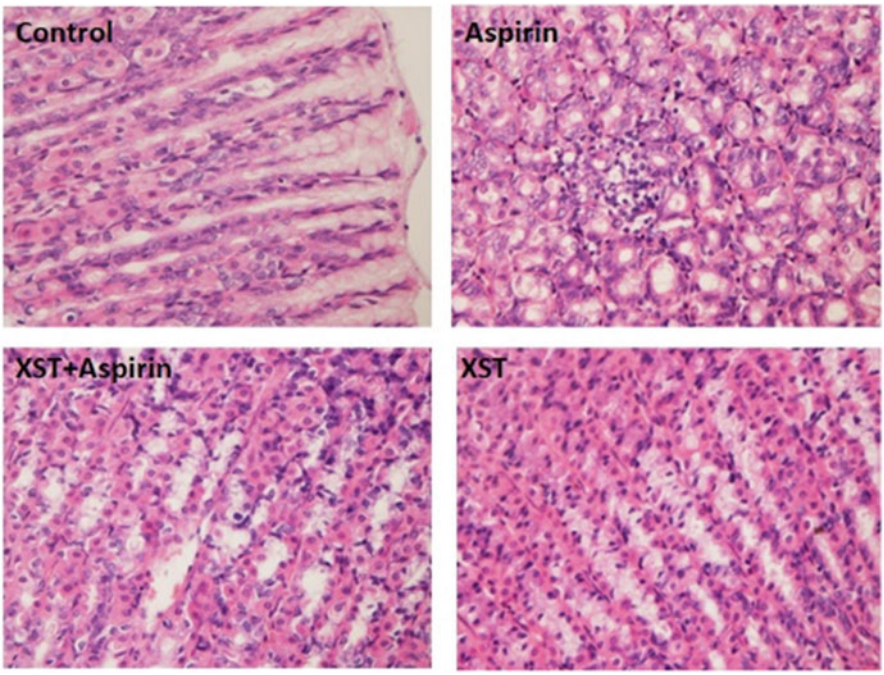

Fig. 7.30 Xuesaitong significantly reduces aspirin-induced gastric mucosal damage in rats

7.4.4.6 Xuesaitong Significantly Reduces Aspirin-Induced Duodenal Microvilli Injury in Rats

As shown in Fig. 7.31, compared with the control group, the number of microvilli on the surface of rat duodenum in the aspirin group significantly reduces. Compared with the aspirin group, Xuesaitong significantly reduces the decrease in microvilli on the duodenum surface induced by aspirin, however, using Xuesaitong alone has no significant effect on microvilli on the surface of rat duodenum.

7.4.4.7 Combined Use of Xuesaitong and Aspirin has Synergistic Effect on the Influence of Gene Expression of MCAO Model Rats

As shown in Fig. 7.32, aspirin has little influence on gene expression of MCAO model rats, while Xuesaitong has significant influence on gene expression of MCAO model rats. The combined use of Xuesaitong and aspirin has synergistic effect on the influence of gene expression of MCAO model rats.

7.4.4.8 Combined Use of Xuesaitong and Aspirin Significantly Affects the Gene Expression of MCAO Model Rats

As shown in Fig. 7.33, compared with the MCAO model group, aspirin causes 58 differential gene expressions, PNS (Panax notoginseng saponins) administration causes 267 differential gene expressions, and ALI Therapy causes 677 differential

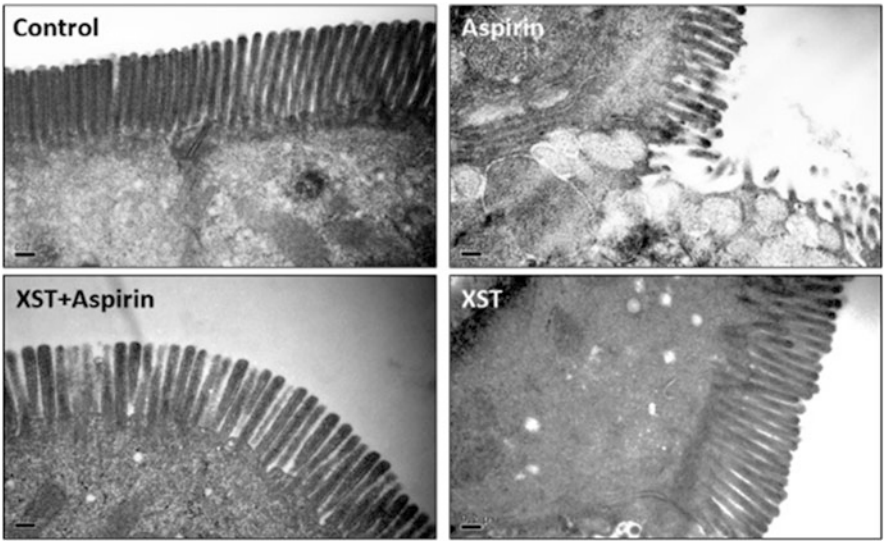

Fig. 7.31 Xuesaitong significantly reduces aspirin-induced duodenal microvilli injury in rats

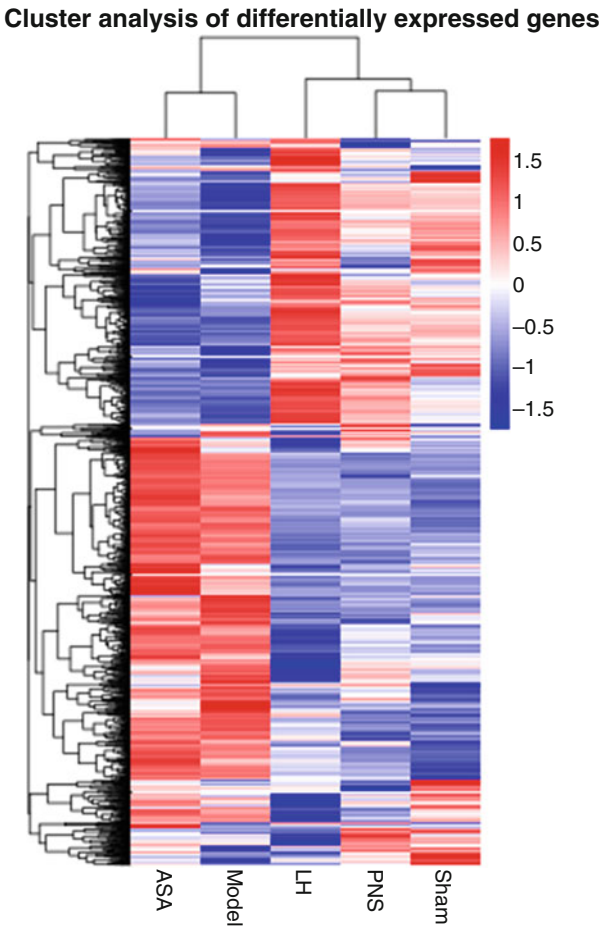

Fig. 7.32 Differential gene cluster diagram of ALI therapy

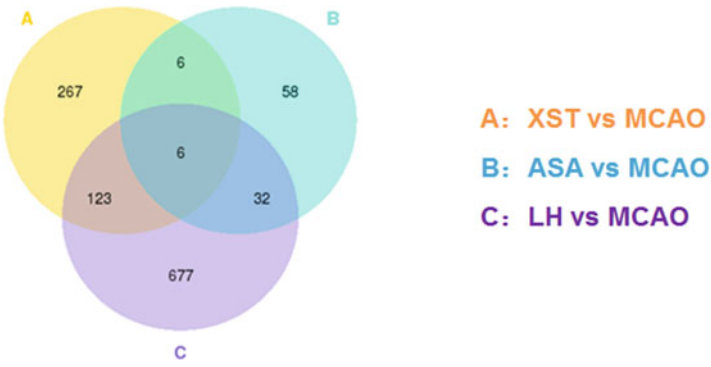

Fig. 7.33 Differential gene venn diagram of ALI therapy

gene expressions; Compared with aspirin, ALI Therapy causes 32 differential gene expressions; Compared with Panax notoginseng saponins, ALI Therapy causes 132 differential gene expressions.

7.4.4.9 Summary

Taking the combined use of Xuesaitong and aspirin as an example, this section comprehensively introduces the experimental ideas and processes of the interaction between TCM and Western medicine based on network pharmacology, and tries to provide reference for the application of network pharmacology in the study of interaction between Chinese and Western medicine. Based on the results of the CTD database and literature research, this section constructs the molecular target networks of Xuesaitong and aspirin in regulating ischemic stroke using network pharmacology. The consistency analysis of the target spectrum of Xuesaitong and aspirin is carried out through the network superposition technology. It was found that there is a high degree of overlap in the ischemic stroke-related genes regulated by aspirin and Xuesaitong. Among the 37 genes regulated by Xuesaitong, 31 genes are completely consistent with those regulated by aspirin, suggesting that the combined use of the two has the potential to enhance the effect of aspirin in the treatment of ischemic stroke. Based on the MCAO/R model of SD rats, we tested the effects of Xuesaitong, aspirin, and Xuesaitong + aspirin on the neurological deficit score and cerebral infarction volume. The results showed that the effect of the combined use of aspirin and Xuesetong is better than using aspirin or Xuesetong alone. In addition, Xuesaitong has a certain alleviating effect on gastrointestinal mucosal damage caused by aspirin or penicillin-streptomycin. In general, based on network pharmacology, this section infers from the drug–target level that the combined use of Xuesaitong and aspirin has the potential to enhance the effect of aspirin in the treatment of ischemic stroke; the network analysis results were verified from the overall level based on the MCAO/R rat model. The experimental results are highly consistent with the network analysis results, indicating that network pharmacology has broad application prospects in explaining the interaction between Chinese and Western medicines.

7.5 Repositioning of Clinical Application of Drugs: New Uses of TCM Ingredients in Protecting Cerebral Ischemia-Reperfusion Injury

Thrombolytic therapy is still the main treatment methodology for acute ischemic stroke. However, cerebral ischemia-reperfusion injury that is a side effect of thrombolytic therapy hinders the successful treatment of acute ischemic stroke. Although reperfusion is the key to the recovery of brain function, reperfusion leads to

excessive production of reactive oxygen species (free radicals), which leads to oxidative stress and further deterioration of brain injury [20]. Elimination of the produced free radicals seems to be a therapeutic strategy for treating acute ischemic stroke. Although pre-clinical experiments proved effective antioxidants that remove active oxygen, the results of clinical trials did not support the same. Nevertheless, the disappointing clinical trial results cannot deny the important role of oxidative stress in cerebral ischemia-reperfusion injury. Targeting the source of free radicals may be a new therapeutic strategy. Although the source of free radicals has not been completely determined, many studies show that NADPH oxidase and mitochondria are the main sources of free radicals in the pathological process of cerebral ischemia-reperfusion [21, 22].

There is increasing evidence that phytoestrogens and notoginseng have protective effects on neurodegenerative diseases including on acute ischemic stroke. Phytoestrogens ginsenoside Rg1 and Rb1 isolated from notoginseng have significant neuroprotective effects on cerebral ischemia-reperfusion injury [23, 24]. Our recent study found that notoginsenoside R1 activates the Akt/Nrf2/HO-1 signaling pathway through an estrogen receptor-dependent pathway and inhibits oxidative stress in PC12 cells [10]. Moreover, HO-1 inhibits the activity of NADPH oxidase and mitochondrial dysfunction [25]. Based on the above research results, we speculate that notoginsenoside R1 may inhibit NADPH oxidase activity and mitochondrial dysfunction by inducing the expression of HO-1, thus playing a neuroprotective role in cerebral ischemia-reperfusion injury.

We used both in vivo and in vitro cerebral ischemia-reperfusion injury models, namely the rat middle cerebral artery occlusion reperfusion model and oxygen glucose deprivation in primary cortical neuronal cells, to evaluate the neuroprotective effects of notoginsenoside R1. In addition, we elucidated the neuroprotective mechanism of Notoginsenoside R1, that is, Notoginsenoside R1 activates Akt/Nrf2 signaling pathway through estrogen receptor-dependent pathway, thus inhibiting NADPH oxidase activity and mitochondrial dysfunction. The research idea and process are shown in Fig. 7.34.

7.5.1 Data Acquisition and Processing

7.5.1.1 Collection of Chemical Component Targets

"Chemicals" was selected under the Keyword Search option of the CTD database, and Notoginsenoside R1 entered in the search box to collect target data of Notoginsenoside R1. "Chemicals" was selected under the Menu option in the ETCM Database menu bar and "Notoginsenoside R1" was entered in the search box, to collect the target data of Notoginsenoside R1. The target data of Notoginsenoside R1 collected from the CTD and ETCM databases were integrated for deduplication processing. The correspondence between Notoginsenoside R1 and its targets was saved in the form of a two-dimensional list.

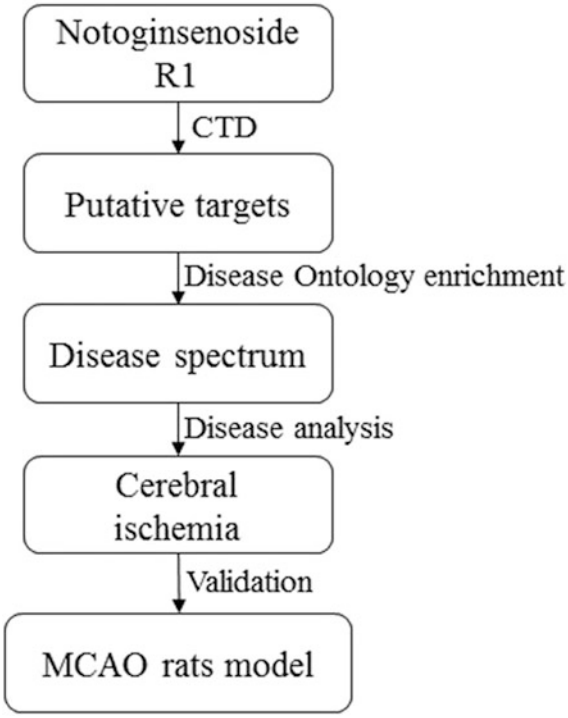

Fig. 7.34 Research ideas and process

7.5.1.2 Disease Ontology Enrichment Analysis

"Set Analyzer" was selected under the Analyze option of the CTD database, "Genes" was selected as the input type, and the abbreviation of the target gene was entered in the input box. "Enriched diseases" was selected as the analysis type, and the corrected P-value threshold was set to 0.01.

7.5.2 Network Construction and Visualization

7.5.2.1 Network Construction and Visualization

The disease spectrum of notoginsenoside R1 obtained through the enrichment analysis of the disease ontology was entered into Cytoscape 3.5.0, to visualize the disease spectrum of notoginsenoside R1. The nervous system diseases and disease-related genes related to notoginsenoside R1 were imported into Cytoscape 3.5.0 to construct a molecular network of "notoginsenoside R1–target–nervous system disease."

7.5.2.2 Analysis Index and Algorithm

The diseases with significant differences were screened and selected according to the corrected p-value (Corrected P-value < 0.01) of each disease in the disease ontology enrichment analysis results.

7.5.3 Network Analysis and Prediction

7.5.3.1 Disease Spectrum Analysis of Notoginsenoside R1

The disease spectrum (as shown in Fig. 7.35) of Notoginsenoside R1 was drawn by selecting the top 60 diseases in the results of disease ontology enrichment analysis, involving 19 disease types (as shown in Fig. 7.36). The top five disease types are cancer, cardiovascular disease, digestive system disease, urogenital disease (male and female), and nervous system disease. In recent years, researchers in China and overseas have reported on the neuroprotective effects of Panax notoginseng,

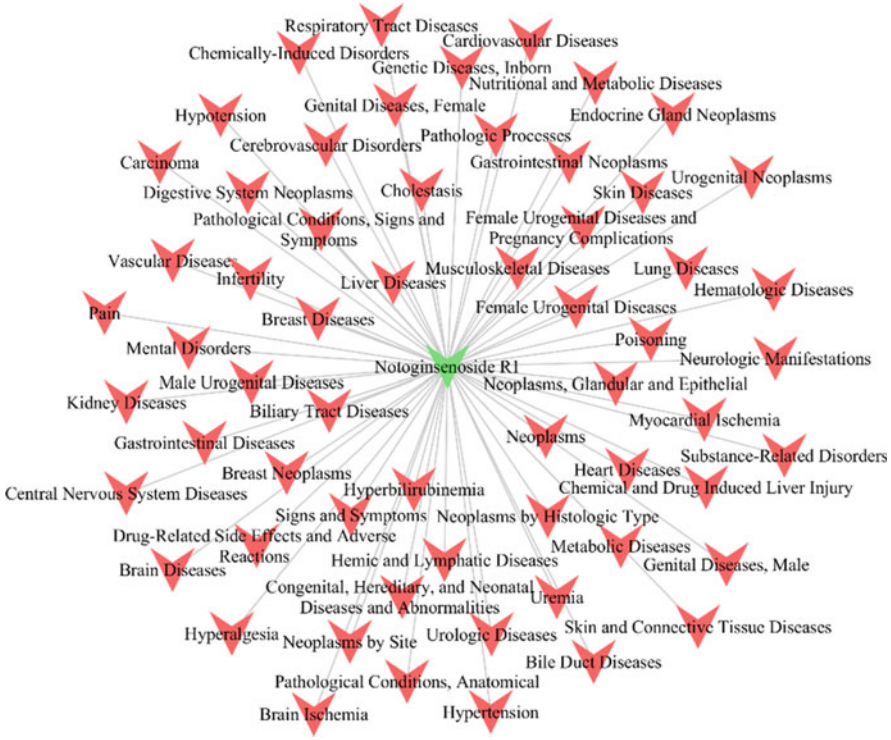

Fig. 7.35 Disease spectrum of notoginsenoside R1. Green and red V-shaped nodes represent Notoginsenoside R1 and diseases related to Notoginsenoside R1, respectively

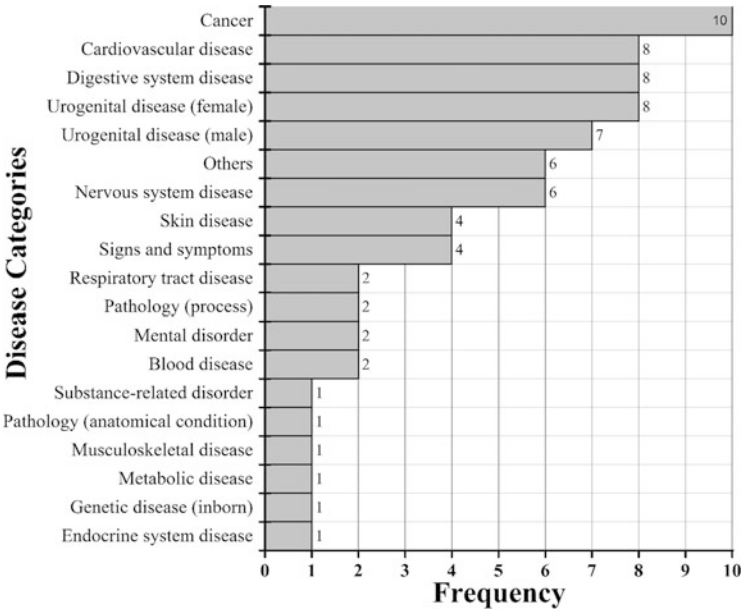

Fig. 7.36 Statistical analysis of panax notoginsenoside R1-related disease types (TOP60). Frequency represents the kinds of diseases involved in each disease type

however, the material basis of neuroprotective activity of Panax notoginseng has not been systematically studied, let alone its mechanism of action. The results of disease spectrum analysis show that Notoginsenoside R1 may play an important role in the neuroprotective effect of Panax notoginseng.

7.5.3.2 Discovery of New Uses of Notoginsenoside R1 in Protecting Cerebral Ischemia-Reperfusion Injury

Figure 7.37 shows the molecular network of Notoginsenoside R1 regulating neurological diseases, the involved disease kinds include cerebral ischemia, cerebrovascular diseases, brain diseases, nervous system manifestations, central nervous system diseases, and hyperalgesia. In addition to cerebral ischemia, the other five disease types (cerebrovascular disease, brain disease, nervous system performance, central nervous system disease, and hyperalgesia) are collectively referred to as a class of diseases. Considering the feasibility and rationality of experimental verification, we next verified the protective effect of Notoginsenoside R1 on cerebral ischemia.

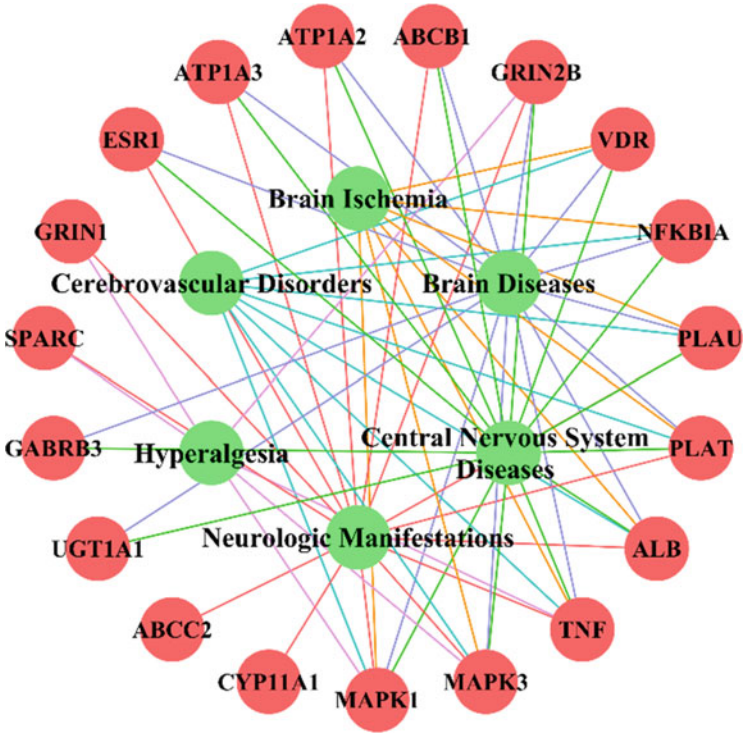

Fig. 7.37 Notoginsenoside R1–target–neural system disease molecular network. The green and red round nodes represent the nervous system diseases related to Notoginsenoside R1 and the nervous system disease-related genes regulated by Notoginsenoside R1, respectively. The orange, blue, red, green, blue, and purple edges are connected to disease genes associated with cerebral ischemia, brain diseases, nervous system manifestations, central nervous system diseases, cerebrovascular disease, and hyperalgesia, respectively

7.5.4 Verification and Summary

7.5.4.1 Notoginsenoside R1 Reduces Neurological Impairment and Cerebral Infarction Volume Caused by Cerebral Ischemia-Reperfusion

It has been reported that Notoginsenoside R1 can reduce the neurological impairment and cerebral infarction volume caused by cerebral ischemia-reperfusion [26]. As shown in Fig. 7.38, the rats in the sham and the NGR1-treated group presented no neurologic deficits and infarction volumes. After 48-h reperfusion, the rats that received I/R treatment displayed a marked increase in neurologic deficit score (Fig. 7.38c, $n = 10$, $P < 0.01$), and a well-defined infarct involving both ischemic core and penumbra (Fig. 7.38a, b, $n = 10$, $P < 0.01$). However, NGR1

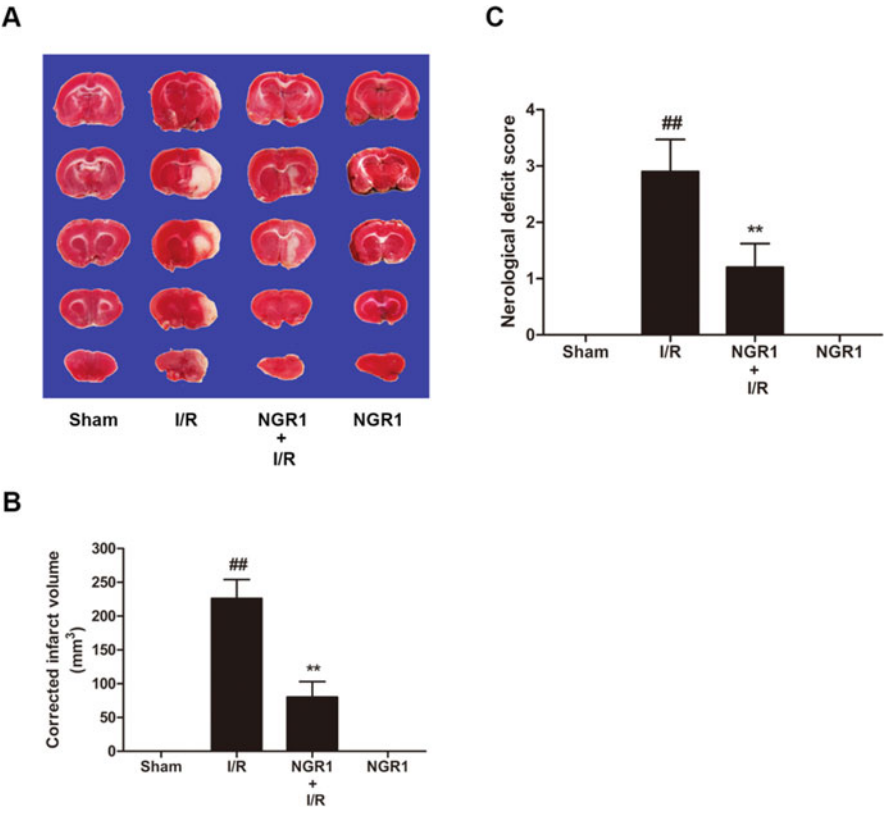

Fig. 7.38 Notoginsenoside R1 reduces neurological impairment and cerebral infarction volume caused by cerebral ischemia-reperfusion. (**a**) TTC staining method to detect cerebral infarction volume. (**b**) Statistical results of cerebral infarction volume. (**c**) Neurological function score

pretreatment provided a significant improvement in neurologic deficit score and remarkably reduced infarct volumes (Fig. 7.38a–c, $n = 10$, $P < 0.01$).

7.5.4.2 Notoginsenoside R1 Increases the Expression of HO-1 in Rat Cerebral Cortex

HO-1 is an antioxidant enzyme with neuroprotective effect. As shown in Fig. 7.39a, b, both histo-cytometer analysis and Western blot analysis show that there are few HO-1 positive cells in the cortex of rats in the sham-operated group, while the expression of HO-1 around the lesions in the I/R model group increases, however, most of them are weak positive cells. Compared with the I/R model group, higher HO-1 level was noted in the NGR1+ I/R group. Interestingly, administration of Notoginsenoside R1 alone significantly increases HO-1 immunoreactivity. We further detected the activity of HO-1. The results show that the HO-1 activity was also

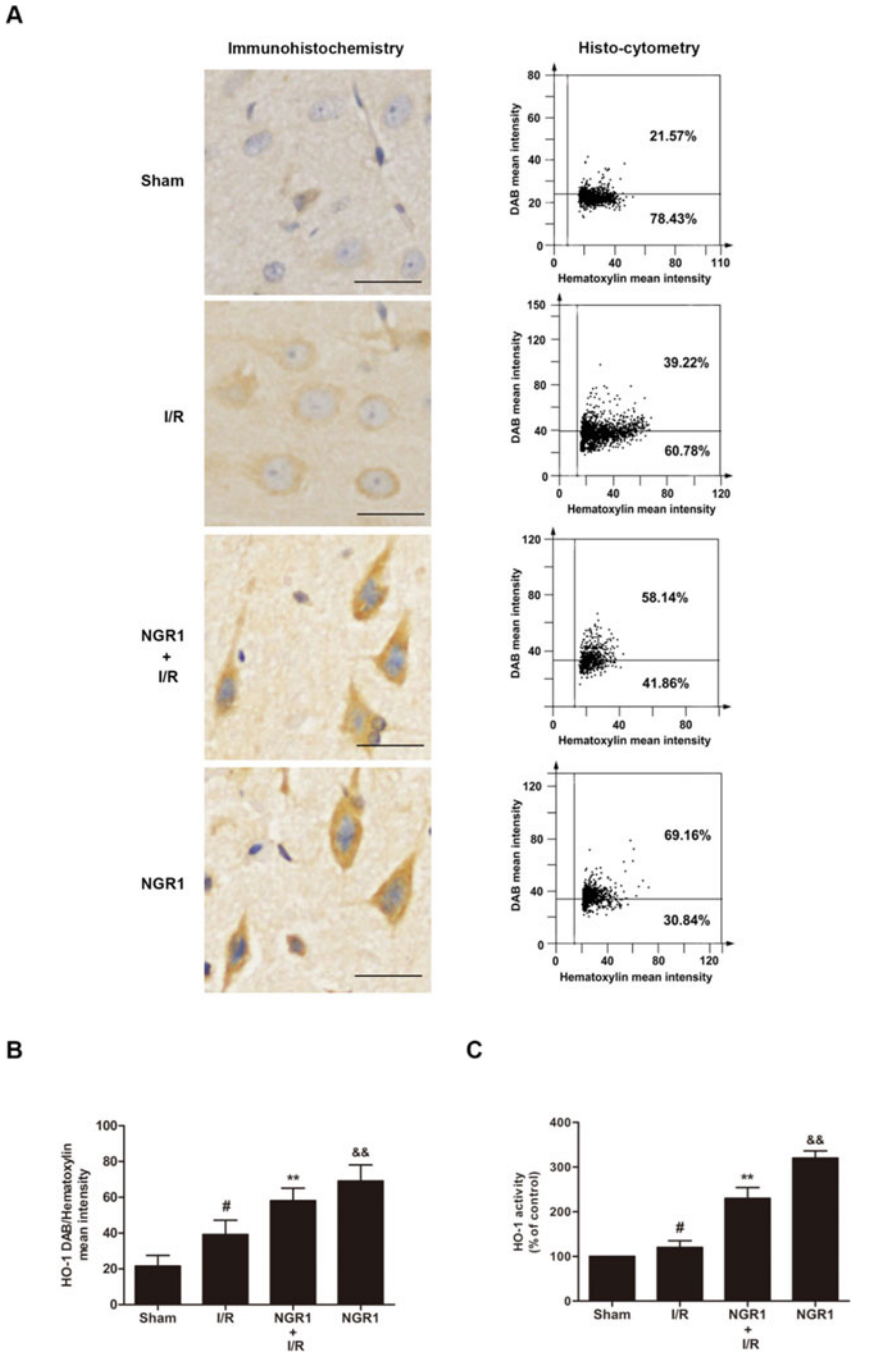

Fig. 7.39 Notoginsenoside R1 increases the expression of HO-1 in rat cerebral cortex. (**a**) Detect the expression of HO-1 in cerebral cortex tissue of rats by immunohistochemistry (left) and analyze the expression level of HO-1 by flow-like analysis (right). (**b**) Statistical map of HO-1 expression

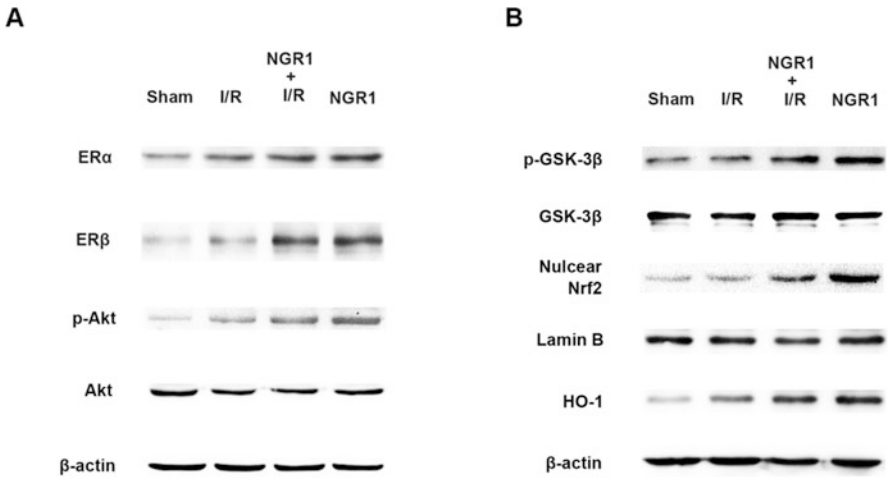

Fig. 7.40 Notoginsenoside R1 activates estrogen receptor-dependent Akt/Nrf2 signaling pathway. (**a**) Notoginsenoside R1 increases the protein expression of ERα and ERβ and the phosphorylation of Akt in the cerebral cortex tissues of rats. (**b**) Notoginsenoside R1 increases the phosphorylation of GSK-3β, accumulation of Nrf2 in nucleus, and protein expression of HO-1 in the cerebral cortex tissues of rats

increased in the I/R, NGR1+ I/R, and NGR1-treated groups (as shown in Fig. 7.39c, $n = 6$, $P < 0.01$).

7.5.4.3 Notoginsenoside R1 Activates Estrogen Receptor-Dependent Akt/Nrf2 Signaling Pathway

Western blot results show that in the I/R model group, the protein expression of HO-1 is significantly up-regulated in the NGR1+ I/R and the NGR1-treated groups, respectively (as shown in Fig. 7.40b, $n = 6$, $P < 0.01$). Moreover, Notoginsenoside R1 significantly increases nuclear accumulation of Nrf2 (as shown in Fig. 7.40b, $n = 6$, $P < 0.01$). We investigated the estrogen receptor and Akt/GSK-3β signaling pathway to clarify the mechanism of Nrf2 activation. As shown in Fig. 7.40a, Notoginsenoside R1 significantly increases the expression of ERα and ERβ proteins and the phosphorylation of Akt and GSK-3β ($n = 6$, $P < 0.01$).

Notosaponin R1 up-regulates HO-1 protein expression and activity by activating the estrogen-receptor-dependent Akt/Nrf2 signaling pathway both in vitro and in vivo, and inhibits NADPH oxidase activity and mitochondrial dysfunction,

Fig. 7.39 (continued) level in cerebral cortex tissue of rats. (**c**) Notoginsenoside R1 increases the activity of HO-1 in cerebral cortex tissue of rats

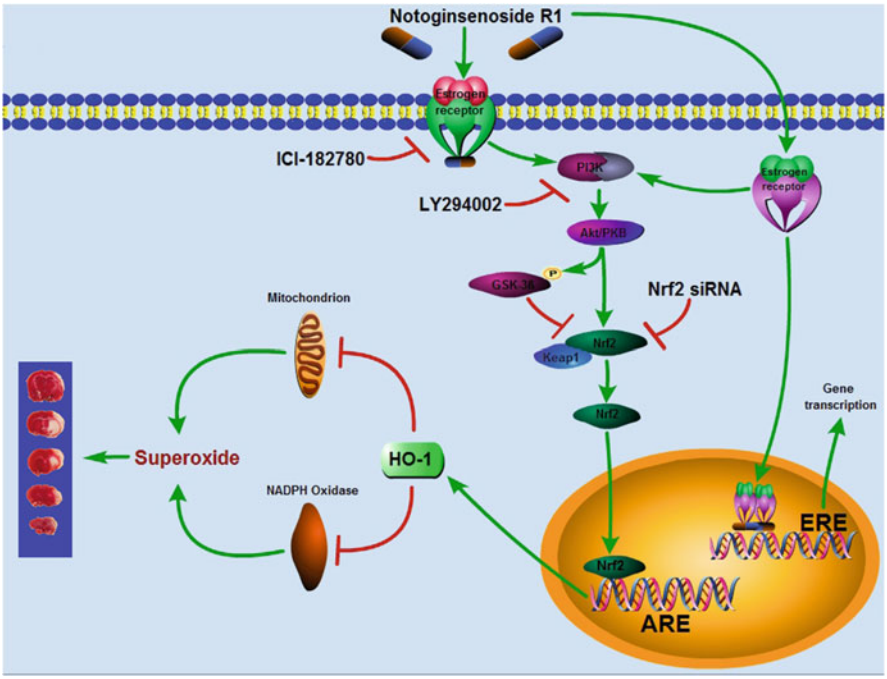

Fig. 7.41 Molecular mechanism illustration of notoginsenoside R1 against cerebral ischemia

thereby inhibiting cerebral ischemia-reperfusion injury and oxygen glucose deprivation reperfusion injury (as shown in Fig. 7.41).

7.5.4.4 Study on Other Mechanisms of the Neuroprotective Effect of Notoginsenoside R1

In-depth studies have been conducted on the neuroprotective mechanism of action of Notoginsenoside R1 in China and overseas. Notoginsenoside R1 activates estrogen receptors, causing crosstalk between Akt and ERK1/2 signaling pathways, thereby activating Nrf2/ARE signaling pathway [10]. Through the estrogen receptor-mediated endoplasmic reticulum, panax Notoginseng saponin R1 stress plays an anti-neonatal cerebral ischemia and hypoxia injury role [27], and the release of stress calcium plays a neuroprotective role by inhibiting the endoplasmic reticulum through PLC [28].

7.5.4.5 Summary

Taking Notoginsenoside R1 as an example, this section comprehensively introduces the experimental ideas and processes of drug repositioning based on network pharmacology, with the aim to provide reference for the application of network pharmacology in drug repositioning research. Based on the CTD database, we collected the target data of Notoginsenoside R1 and predicted the disease spectrum of Notoginsenoside R1 through disease ontology enrichment. The results of disease ontology enrichment indicate that Notoginsenoside R1 has protective effect on nervous system diseases such as cerebral ischemia. To investigate the reliability of the prediction results, we tested the protective effect of Notoginsenoside R1 on cerebral ischemia based on the MCAO model. The results show that: Notoginsenoside R1 activates the Akt/Nrf2/HO-1 pathway in an estrogen receptor-dependent manner, and inhibits NADPH oxidase activity and mitochondrial dysfunction, thereby inhibiting the production of peroxides, and finally plays a neuroprotective role in cerebral ischemia-reperfusion injury. In general, based on network pharmacology, this section predicts the disease spectrum of Notoginsenoside R1, and discovers a new use of Notoginsenoside R1 in protecting against cerebral ischemia. This use of Notoginsenoside R1 has been verified on the MCAO model, indicating that network pharmacology is an effective method and strategy for drug relocation research.

7.6 Development of Multi-target Drugs: Low-Density Lipoprotein-Induced Endothelial Cell Injury Protected by Synergistic Compatibility of TCM Ingredients

As a complex disease, the occurrence and development of atherosclerosis involves multiple targets, and the commercially available single-target drugs have limited therapeutic effects [29]. The traditional drug development concept of "one gene, one disease, one drug" is facing great challenges in the prevention and treatment of atherosclerosis. In recent years, the rise of the "multi-gene, multi-target" drug development model has pointed the way for new drug development in atherosclerosis. TCM has rich practical experience in the treatment of complex diseases, and has been widely recognized for its multi-channel, multi-target, and low toxicity treatment features. However, due to the complex ingredients, slow onset of action, difficulty in quality control, and lack of systematic toxicological studies, it is difficult to determine the material basis of its efficacy. Both, the unclear mechanism of action, and unclear target of action, limit the promotion and application of TCM in the international community. Therefore, developing innovative TCM prescriptions with definite curative effect, controllable quality, and clear mechanism of action has become a critical requirement in the treatment of atherosclerosis.

Network pharmacology is a novel method developed on the basis of systems biology and multidirectional pharmacology [30]. By integrating the drug–target protein interaction network and the biological network, it analyzes the interaction between drugs and other nodes in the network, and then analyzes the effectiveness and toxicity of drugs. Guanxin Danshen Formulation is an effective prescription for the treatment of coronary cardiovascular diseases developed by our research group. It is mainly composed of three herbs: Salvia miltiorrhiza, Panax notoginseng, and Dalbergia odorifera. Clinically, it is effective in treating coronary cardiovascular disease caused by qi stagnation and blood stasis, but there have been few studies on its efficacy in treating atherosclerosis. In recent years, relevant experimental studies have shown that salvianolic acid B, the main water-soluble component of Salvia miltiorrhiza, can effectively reduce blood lipids, reduce lipid content in plaque, reduce plaque area, increase fiber thickness, and reduce plaque erosion and angiogenesis in plaque [31], thus effectively preventing the occurrence of atherosclerosis and stabilizing atherosclerotic plaque. Although ginsenoside Re in Panax notoginseng has not been reported directly in the prevention and treatment of atherosclerosis, it can effectively reduce the content of malondialdehyde (MDA), enhance the activities of superoxide dismutase (SOD) and glutathione (GSH-Px), reduce the release of lactate dehydrogenase (LDH), and enhance the scavenging of DPPH free radicals, thereby reducing oxidative damage. In addition, ginsenoside Re effectively reduces the secretion of IL-6, TNF-α, IL-10, and other related inflammatory factors in serum, and inhibit inflammation [32]. The role of ginsenoside Re in regulating apoptosis-related proteins has also been reported. [33] Previous studies suggest that ginsenoside Re can exert anti-atherosclerotic effects through its anti-inflammatory, antioxidant, and anti-apoptotic effects.

Based on network pharmacology, this section investigates the overall protective effect of salvianolic acid B (Sal B) and ginsenoside Re (Re) on oxidative low-density lipoprotein (Ox-LDL)-induced injury of human umbilical vein endothelial cells (HUVECs) through multiple targets and pathways.

7.6.1 Data Acquisition and Processing

First, the pathological database of atherosclerosis, the Ox-LDL-induced HAEC cell damage expression profile database, and the Ox-LDL-induced HUVECs damage protein chip database were constructed. Then, using the molecular docking technology combined with literature statistics, the direct-action targets of salvianolic acid B and ginsenoside Re were determined. The targets of salvianolic acid B (Sal B) and ginsenoside Re (RE) were imported into the constructed disease pathology database, to find overlapping targets. Finally, through relevant GO function annotation, KEGG pathway analysis, and protein interaction analysis the mechanism of action of the two compounds' cooperative protection of Ox-LDL-induced HUVECs damage was explored, to provide research ideas and technical support for the in-depth development of Guanxin Danshen Formulation (as shown in Fig. 7.42).

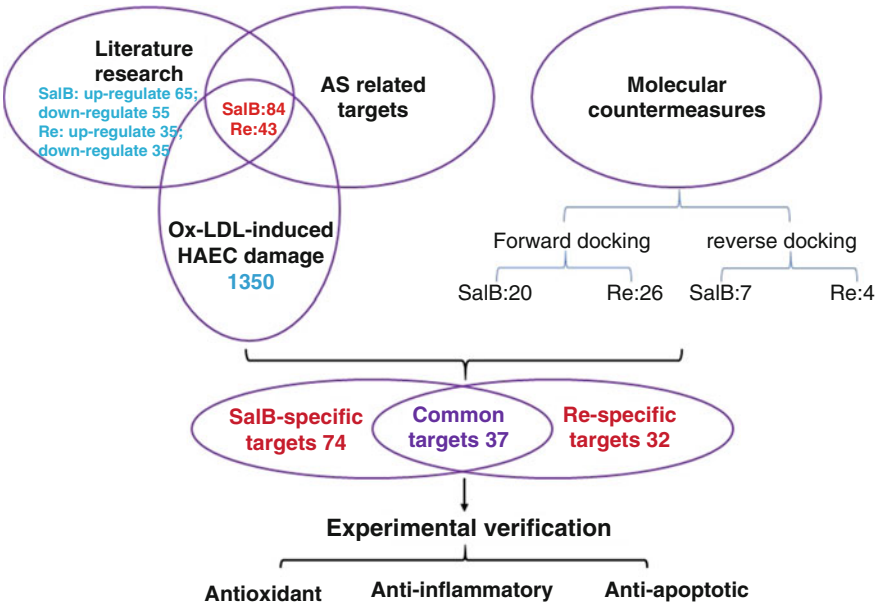

Fig. 7.42 Research ideas and processes

7.6.1.1 Collection of Chemical Component Targets

Using salvianolic acid B and ginsenoside Re as keywords, we searched the CNKI, Pubmed, SCI, ScienceDirect, and Springer databases to obtain related literature on salvianolic acid B and ginsenoside Re. The end date for the literature search was 2016-6-17. We extracted the relevant targets of salvianolic acid B and ginsenoside Re by reading the full text. We used PharmMapper and idTarget to predict the potential action targets of salvianolic acid B and ginsenoside Re, and all the docking parameters were set according to the default values on the website. Finally, we integrated the literature search results with the molecular docking prediction results.

7.6.1.2 Atherosclerosis-Related Genes

We searched genes related to atherosclerosis diseases based on the GeneCards database, the end date was 2016-6-30.

7.6.1.3 Differential Gene Analysis Based on Gene Expression Profile

We downloaded GSE13139 gene expression profile data based on NCBI's GEO database. This group of data contains five groups of data: inducing HAEC cell damage without adding Ox-LDL, and inducing HAEC cells for 2 h, 6 h, 12 h, and

24 h with Ox-LDL. The data was normalized based on the R language bioconductor toolkit, and differentially expressed genes were determined.

7.6.1.4 Analysis of Apoptosis Targets and Inflammatory Factors in Ox-LDL-Induced HUVECs Damage

This part mainly includes the data on apoptosis and inflammatory factors: inducing HUVECs cell damage without adding Ox-LDL and inducing HUVECs cells for 12 h with Ox-LDL. Human apoptotic protein chip (RayBiotech, USA) and human inflammatory factor protein chip (RayBiotech, USA) were used to detect apoptotic proteins and inflammatory factors.

7.6.2 Network Construction and Visualization

Each network involved in this study was drawn by using Cytoscape 3.5.0.

7.6.2.1 GO Function Enrichment Analysis

The online enrichment analysis tool DAVID was used to perform Gene Ontology (GO) enrichment analysis. GO enrichment analysis mainly includes three parts: Molecular Function (MF), Cellular Component (CC), and Biological Process (BP).

7.6.2.2 KEGG Pathway Analysis

In this experiment, the Cluster Profiler package and Kobas2.0 were used to analyze the KEGG pathway of target genes, and the obtained data were imported into Cytoscape, to construct the compound–target gene–pathway–disease network diagram.

7.6.2.3 Analysis Index and Algorithm

Differential gene expression analysis, KEGG analysis, and GO function analysis all use false discovery rate (FDR) test. When FDR< 0.05 or $P < 0.05$, the difference is considered significant and statistically significant.

7.6.3 Network Analysis and Prediction

7.6.3.1 Statistics of Potential Target Genes on the Protective Effects of SalB and Re on Ox-LDL-Induced Endothelial Cell Damage

After standardizing the targets of salvianolic acid B and ginsenoside Re retrieved from CNKI, Pubmed, SCI, ScienceDirect, and Springer databases by NCBI gene data and correlated with protein chip data, 120 target genes related to salvianolic acid B and 70 target genes related to ginsenoside Re were finally obtained. The obtained target genes were correlated with the atherosclerotic disease gene library and the differential genes of Ox-LDL-induced HAEC cell damage; the overlapping target genes were removed, and finally there are 84 target genes related to salvianolic acid B and 43 target genes related to ginsenoside Re [32].

According to the pharmacophore simulation docking and reverse docking, two molecular docking databases of both salvianolic acid B and ginsenoside Re were obtained. According to the scoring and ranking rules of their respective websites, the top 100 proteins with the docking scores were taken, and their protein names were converted into gene names, and finally associated with the atherosclerosis disease gene library, to find the overlapping parts. Finally, 27 target genes related to salvianolic acid B and 30 target genes of ginsenoside Re were obtained.

By integrating the target genes and molecular docking results of database three, a total of 111 target genes related to salvianolic acid B and 69 target genes of ginsenoside Re were obtained. Further analysis shows that salvianolic acid B and ginsenoside Re have a common target gene 37. Therefore, the specific target of salvianolic acid B is 74, and the specific target gene of ginsenoside Re is 32.

7.6.3.2 Go Enrichment Analysis of Potential Target Genes on the Protective Effects of SalB and Re on Ox-LDL-Induced Endothelial Cell Damage

First, the GO function enrichment analysis on the common target genes between salvianolic acid B and ginsenoside Re was performed, and the common 37 target genes between them were imported into the DAVID web database. A total of 376 annotations were obtained with respect to cell components, molecular functions, and biological processes. With FDR < 0.05 as the screening condition, 69 annotations were finally obtained. As shown in Fig. 7.43, the common target genes mainly play an antioxidant role in the cell fluid and extracellular sites. The biological process mainly involves antioxidant, anti-apoptotic, and maintenance of cell ion balance; the key genes are GPX and SOD.

Next, the GO function enrichment analysis was performed on the specific target genes of salvianolic acid B, and its specific 74 target genes were imported into the DAVID web database. A total of 684 annotations were obtained with respect to cell components, molecular functions, and biological processes. With FDR < 0.05 as the

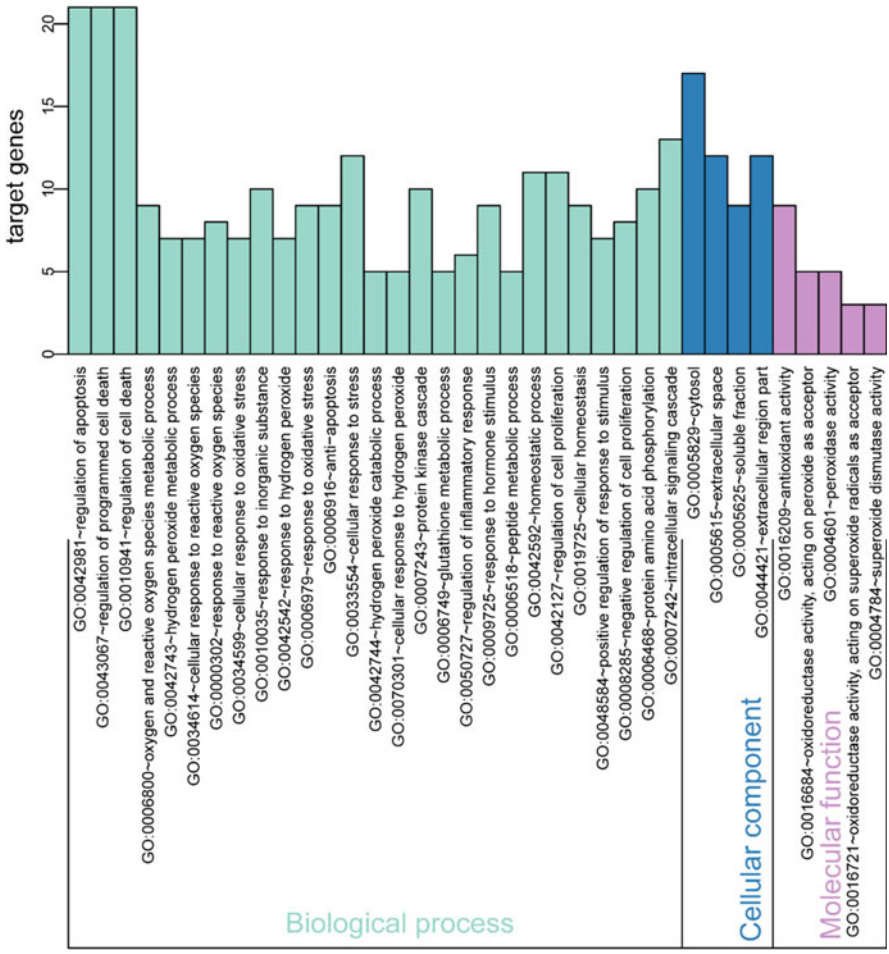

Fig. 7.43 GO function enrichment analysis on the common target genes between salvianolic acid B and Ginsenoside Re

screening condition, 113 annotations were finally obtained. As shown in Fig. 7.44, the common target genes mainly play antioxidant and electron transport functions in the cytoplasmic membrane and extracellular sites, and biological processes mainly involve antioxidant, cell proliferation, cell migration, anti-inflammatory, and other functions; the key genes are GSR, NOX5, NOX1, and NOS3.

Lastly, the GO function enrichment analysis was performed on the specific target genes of ginsenoside Re, and the specific 32 target genes were imported into the DAVID web database. A total of 282 annotations were obtained with respect to cell components, molecular functions, and biological processes. With FDR < 0.05 as the screening condition, 16 annotations were finally obtained. As shown in Fig. 7.45, the common target genes mainly play the role of steroid hormone in cell processes, and

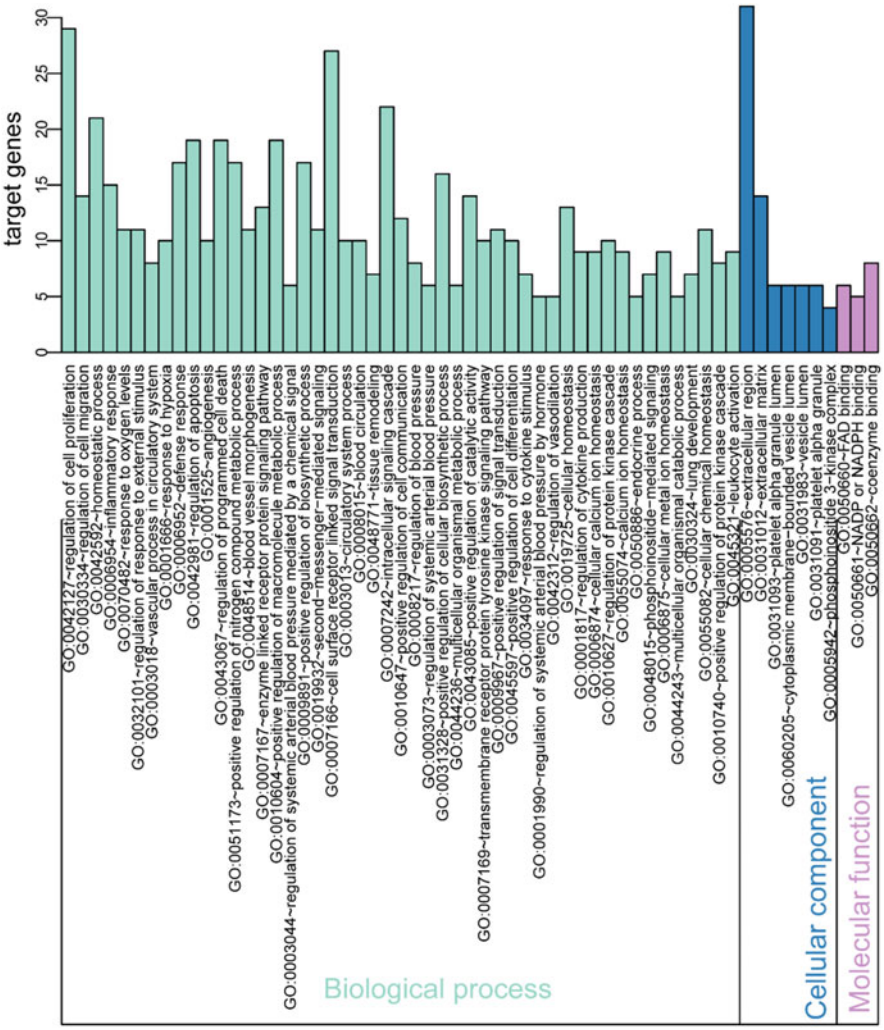

Fig. 7.44 GO function enrichment analysis on the specific target genes of salvianolic acid B

the main biological processes mainly involve hormone stimulation, cell proliferation, insulin stimulation, etc.; the key genes are AR, RXRB, RXRA, ESR1, and ESR2.

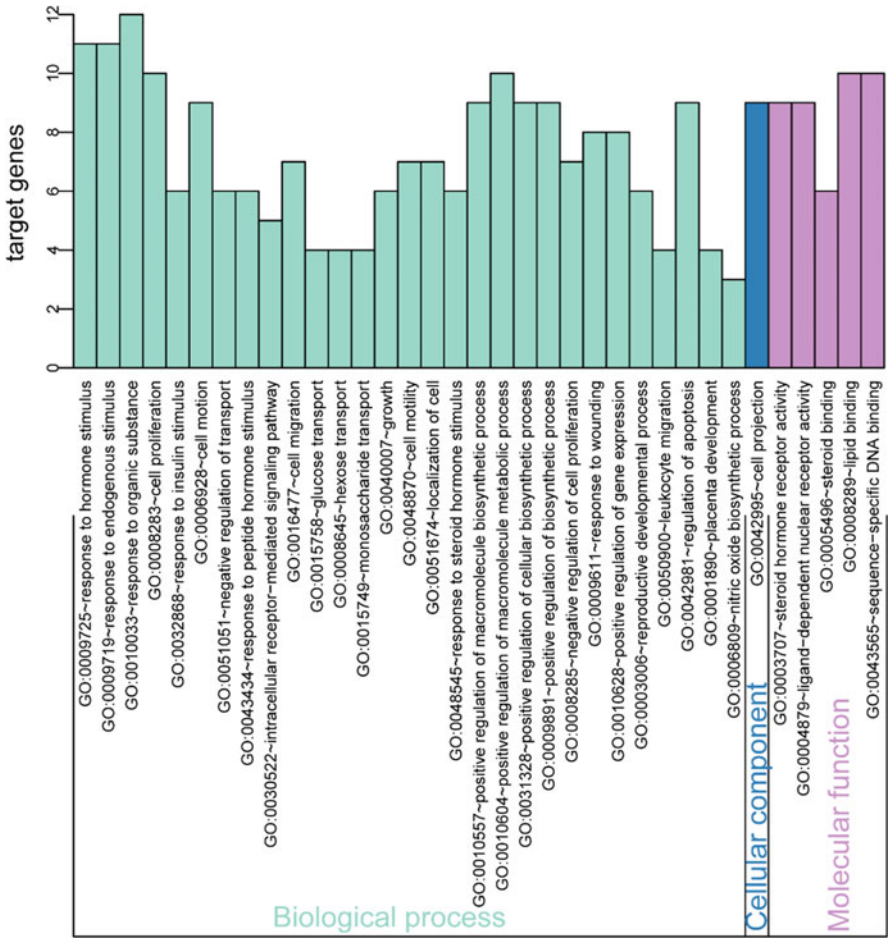

Fig. 7.45 GO function enrichment analysis on the specific target genes of ginsenoside Re

7.6.3.3 KEGG Pathway Analysis of Potential Target Genes on the Protective Effects of SalB and Re on Ox-LDL-Induced Endothelial Cell Damage

First, KEGG Pathway analysis was performed on the common target genes between salvianolic acid B and ginsenoside Re, and the common 37 target genes between them were imported into the Cluster Profiler package and Kobas 2.0, using FDR $<$ 0.05 or $P < 0.05$ as the screening condition. The results are shown in Fig. 7.46. These target genes are mainly enriched in Toll-like receptor pathway, NF-κB pathway, MAPK signaling pathway, viral and bacterial disease-related pathway, and energy metabolism. The 37 target genes are involved in a total of 71 pathways, and many genes are involved in multiple signaling pathways concurrently. For

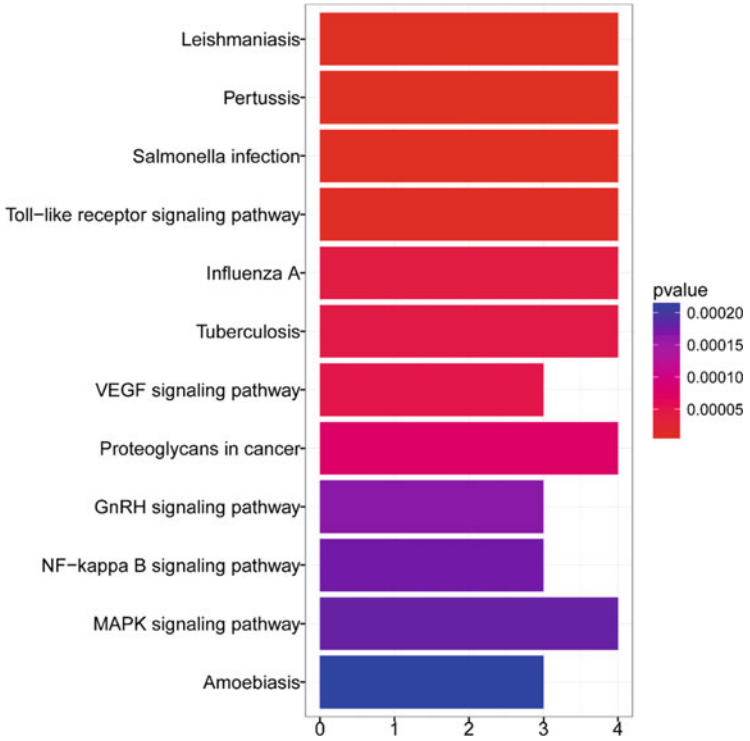

Fig. 7.46 KEGG pathway analysis of the common target genes between salvianolic acid B and Ginsenoside Re

example, CD14 gene plays a role in Toll-like receptor pathway, NF-κB pathway, and MAPK signaling pathway.

Next, the KEGG Pathway analysis was performed on the specific target genes of salvianolic acid B, and the specific 74 target genes were imported into the Cluster Profiler package and Kobas 2.0, using FDR < 0.05 or $P < 0.05$ as the screening condition. The results are shown in Fig. 7.47. These target genes are mainly enriched in TNF signaling pathway, AGE-RAGE signaling pathway, Ras signaling pathway, monocyte migration, and local adhesion signaling pathways. The 74 target genes are involved in a total of 34 pathways, and many genes are involved in multiple signaling pathways concurrently. For example, PIK3CD gene plays a role in Toll-like receptor pathway, TNF signaling pathway, and AGE-RAGE signaling pathway.

Last, the KEGG Pathway analysis was performed on the specific target genes of ginsenoside Re, and the specific 32 target genes were imported into the Cluster Profiler package and Kobas 2.0, using FDR < 0.05 or $P < 0.05$ as the screening condition. The results are shown in Fig. 7.48. These target genes are mainly enriched in adipocytokine signaling pathway, hormone signaling pathway, insulin resistance signaling pathway, and PPAR signaling pathway. The 32 target genes are involved in a total of 21 pathways, and many genes are involved in multiple signaling

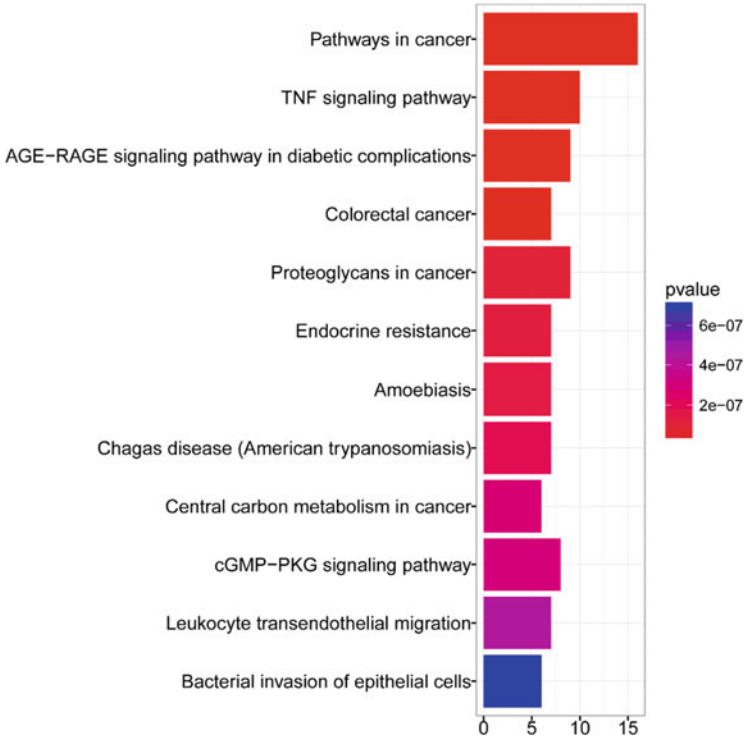

Fig. 7.47 KEGG pathway analysis of the specific target genes of salvianolic acid B

pathways concurrently. For example, RXRB gene plays a role in adipocytokine signaling pathway, hormone signaling pathway, insulin resistance signaling pathway, and PPAR.

7.6.3.4 Related Network Construction and Analysis of Potential Target Genes on the Protective Effects of SalB and Re on Ox-LDL-Induced Endothelial Cell Damage

Drug targets are the active sites of direct action of drugs in organisms, including gene sites, nucleic acids, various enzymes, ion channels, membrane proteins, and other biological macromolecules. Strictly speaking, drug targets refer to biomacromolecules with specific drugs in the market. The key to new drug research and development is to determine potential drug targets and lead compounds, which is also the key to researching drug molecules that can play a role in the treatment of diseases. In this experiment, Cytoscape 3.4.0 was used to construct and analyze the "compound–target–pathway–disease" network by analyzing the common and specific target gene pathway annotations and corresponding diseases of salvianolic acid B and ginsenoside Re. The network map of specific target genes shows that there are

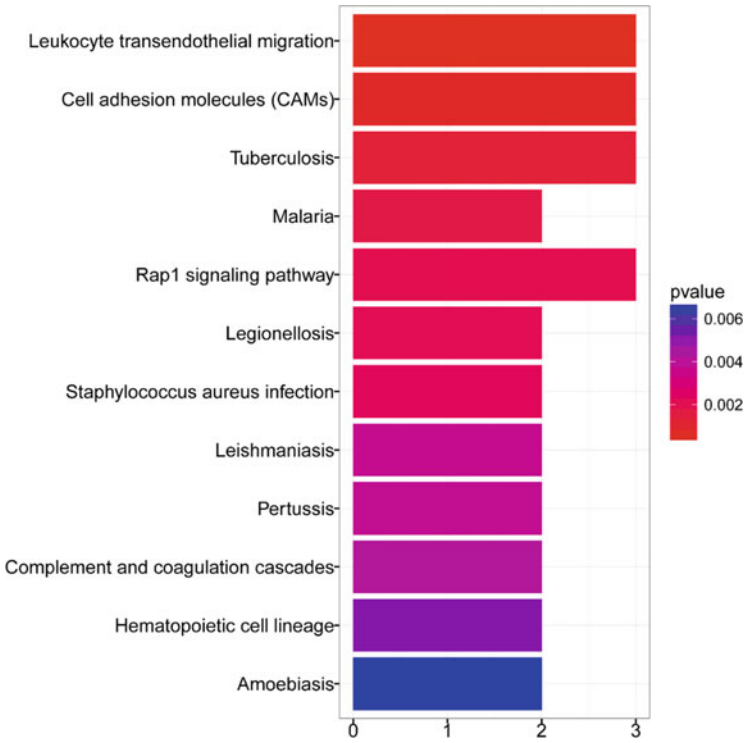

Fig. 7.48 KEGG pathway analysis of the specific target genes of Ginsenoside Re

five target genes that are only involved in the regulation of pathways, but not that of cardiovascular-related diseases; 23 genes are only involved in regulating cardiovascular diseases, without specific pathway positioning; and there are 9 genes involved in both regulation of cardiovascular disease and that of related pathways (as shown in Fig. 7.49) [32].

Next, the "compound–target–pathway–disease" network of each specific target gene of salvianolic acid B and ginsenoside Re was analyzed. The results are shown in Fig. 7.50 [32]. The regulation pathways of specific target genes of salvianolic acid B and ginsenoside Re and diseases have both commonness and specificity. They both regulate insulin resistance and monocyte migration-related pathways and immune-related diseases. The difference is that the regulation pathway of salvianolic acid B is mainly related to the inflammation and energy metabolism, while ginsenoside Re focuses on regulating the signal pathway related to fat metabolism. In terms of disease regulation, salvianolic acid B mainly regulates cardiovascular diseases, but ginsenoside Re mainly regulates vascular inflammation diseases.

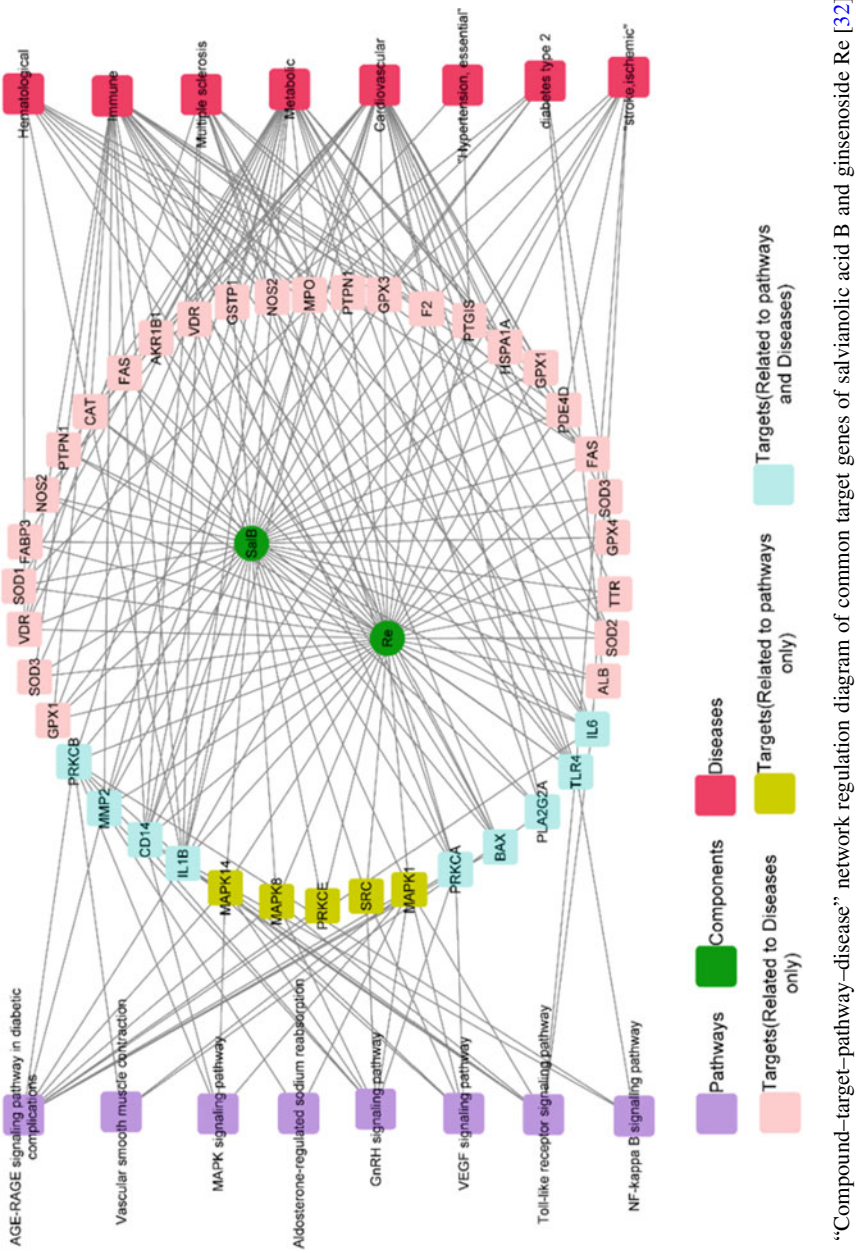

Fig. 7.49 "Compound–target–pathway–disease" network regulation diagram of common target genes of salvianolic acid B and ginsenoside Re [32]

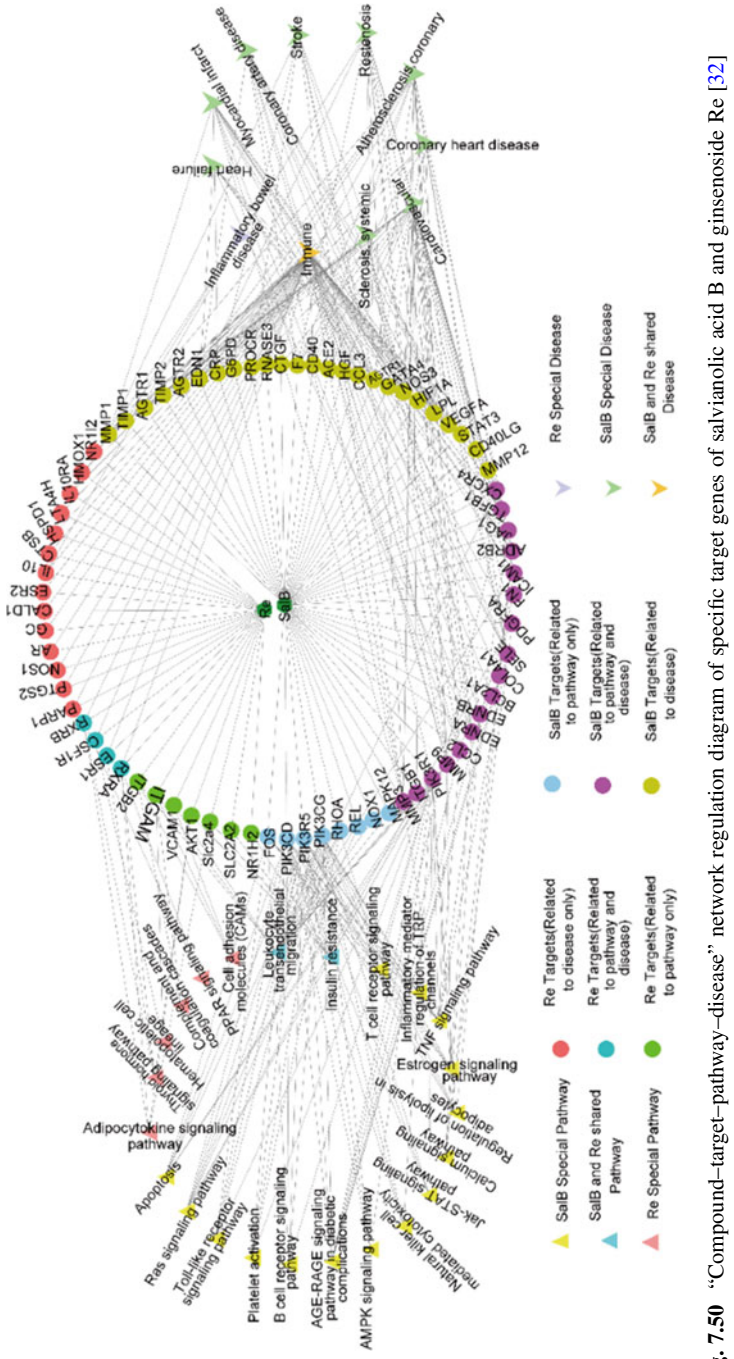

Fig. 7.50 "Compound–target–pathway–disease" network regulation diagram of specific target genes of salvianolic acid B and ginsenoside Re [32]

7.6.4 Verification and Summary

Network pharmacology was used to mine the action target information of salvianolic acid B and ginsenoside Re. The results revealed the mode of action between salvianolic acid B and ginsenoside Re synergy anti-Ox-LDL-induced HUVECs injury through multi-targets and multi-pathways, at the molecular network level. The molecular mechanism of salvianolic acid B and ginsenoside Re in synergistic protection of ox-LDL-induced HUVECs injury through multi-targets and multi-pathways was verified in vitro.

7.6.4.1 SalB, Re, and SR Inhibited Ox-LDL-Induced HUVECs Oxidative Stress Injury

In this study, flow cytometry was used to analyze the effects of Ox-LDL-induced intracellular ROS levels in HUVECs. The experimental results show that after Ox-LDL treatment, intracellular ROS levels increase significantly, which is manifested by increased fluorescence of carboxy-H2DCF (Fig. 7.51a) [32]. The statistical results (Fig. 7.51b) show that compared with the control group, Ox-LDL treatment can cause significant increase in the intracellular ROS level. Compared with the model group, the intracellular ROS levels of SalB, Re, and SR pretreatment decrease significantly. However, the SR group has the strongest inhibitory effect on ROS production in Ox-LDL-induced HUVECs, which is more statistically significant compared with the two monomers. Between the two monomers, the inhibitory effect of SalB on ROS in HUVECs is stronger than that of Re (Fig. 7.51b) [32].

Intracellular antioxidant enzyme activity detection showed that compared with the control group, the Ox-LDL treatment caused a significant decrease in intracellular CAT, SOD, and GSH-Px enzyme activities; compared with the model group, the activities of CAT, SOD, and GSH-Px increase after pretreatment with SalB, Re, and SR. The enhanced enzyme activities of CAT, SOD, and GSH-px in the SR group are stronger than those of the two monomers, between the two monomers, the enhancing effect of SalB on CAT, SOD, and GSH-Px-enhanced enzyme activities is stronger than that of Re (Fig. 7.51c–e) [32]. The results of intracellular antioxidant enzyme activities are consistent with the results of intracellular ROS level detection.

7.6.4.2 Effects of SalB, Re, and SR on the Expression of Cytoinflammatory Factors and Adhesion Molecules in HUVECs Damage Induced by Ox-LDL

In this study, the ELISA method was used to analyze the expression of inflammatory factors in HUVECs cells induced by Ox-LDL. The research results show that the secretion of inflammatory factors IL-6 and TNF-α in the cells increases significantly after Ox-LDL treatment. Compared with the model group, the secretion of

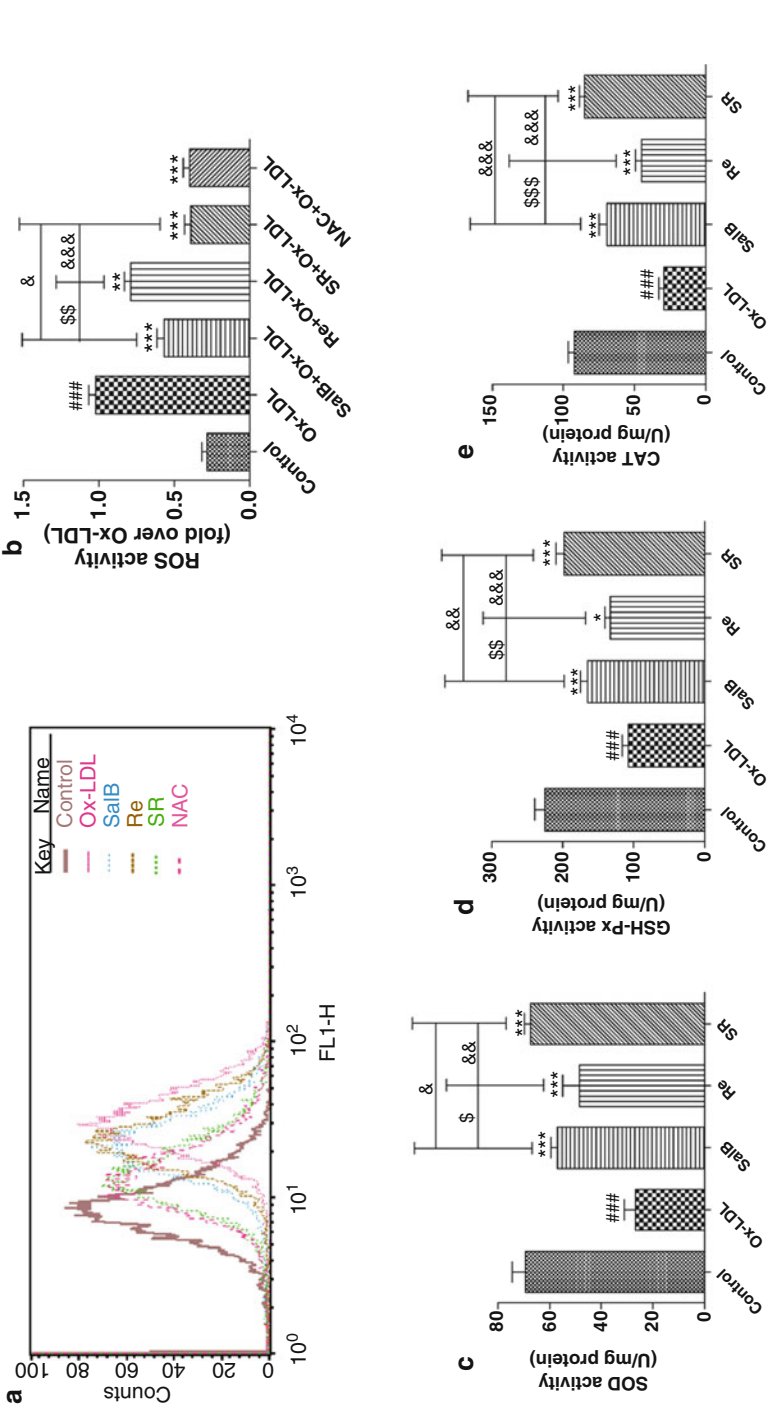

Fig. 7.51 Protective effects of SalB, Re, and SR on Ox-LDL-induced oxidative stress in HUVECs [32]. (**a**) Protective effect of SalB, Re, and SR pre-incubation for 12 h on Ox-LDL-induced over-production in HUVECs cell ROS; (**b**) Statistical diagram of ROS over-production in HUVECs cells induced by Ox-LDL; (**c**) Protective effect of SalB, Re, and SR pre-incubation for 12 h on Ox-LDL-induced production in HUVECs cell SOD; (**d**) Protective effect of SalB, Re, and SR pre-incubation for 12 h on Ox-LDL-induced production in HUVECs cell GSH-Px; (**e**) Protective effect of SalB, Re, and SR pre-incubation for 12 h on Ox-LDL induced production in HUVECs cell CAT. $^{***}P < 0.001$, $^{**}P < 0.01$, $^{*}P < 0.05$ compared with Ox-LDL; $^{\#\#\#}P < 0.001$ compared with Control; $^{\$\$\$}P < 0.001$, $^{\$\$}P < 0.01$, $^{\$}P < 0.05$ and SalB; $^{\&\&\&}P < 0.001$, $^{\&\&}P < 0.01$, $^{\&}P < 0.05$ compared with SR

intracellular inflammatory factors significantly reduces after SalB, Re, and SR pretreatment. However, the SR group has the strongest reducing effect on the secretion of inflammatory factors, followed by SalB, and Re, which is the weakest. The comparison between every neighboring two groups is statistically significant (as shown in Fig. 7.52a–c) [32].

Western blot is used to study the effects of SalB, Re, and SR on the expression of adhesion molecules (as shown in Fig. 7.52d–f). Compared with the control group, Ox-LDL significantly up-regulates the expression of adhesion molecules ICAM-1 and VCAM-1, while SalB and SR pretreatment can reverse the expression of ICAM-1 and VCAM-1. When adding p38MAPK agonist and PI3K inhibitor, it can block the protective effects of SalB and SR. Studies have shown that Re has no effect on the expression of adhesion molecules ICAM-1 and VCAM-1 [32]. At the same time, the results of MCP-1 secretion analysis using the ELISA method show that after Ox-LDL treatment, intracellular MCP-1 secretion increases significantly. Compared with the model group, the secretion of intracellular MCP-1 reduces significantly after SalB, Re, and SR pretreatment. However, the SR group has the strongest reducing effect on the secretion of MCP-1, followed by SalB, and Re, which is the weakest. Re has a significant effect on the secretion of McP-1, and the comparison between every neighboring two groups is statistically significant.

7.6.4.3 SalB, Re, and SR Regulate the Expression of Apoptosis-Related Proteins in the Damage Process of Ox-LDL-Induced HUVECs Through PI3K/Akt Pathway and p38MAPK/NF-κB Pathway

Western blot is used to study the effects of SalB, Re, and SR on apoptosis-related protein expression (as shown in Fig. 7.53a–d) [32]. Compared with the blank control group, Ox-LDL significantly inhibits the expression of anti-apoptotic proteins Bcl-2 and cIAP2. While up-regulating the expression of pro-apoptotic protein Bax and Smac and down-regulating the ratio of Bcl-2/Bax, the pretreatment with SalB, Re, and SR significantly inhibits the effect of Ox-LDL on Bcl-2 family proteins. Increasing the ratio of Bcl-2/Bax and reversing the expression of cIAP2 and Smac, the SR group has strongest regulatory effect, followed by SalB group, and the Re group being the weakest, however, they all have significant differences. After adding PI3K-specific inhibitor LY294002 or p38MAPK agonist, the regulatory effect of SR on apoptosis protein expression in HUVECs significantly reduces, thus suggesting that the regulation of SR on apoptotic proteins in HUVECs' injury induced by OX-LDL is regulated by the PI3K/Akt pathway and the p38MAPK/NF-κB pathway. At the same time, SalB, Re, and SR can inhibit the increased activity of the pro-apoptotic protein cleaved Caspase3 caused by Ox-LDL (as shown in Fig. 7.53e, f) [32].

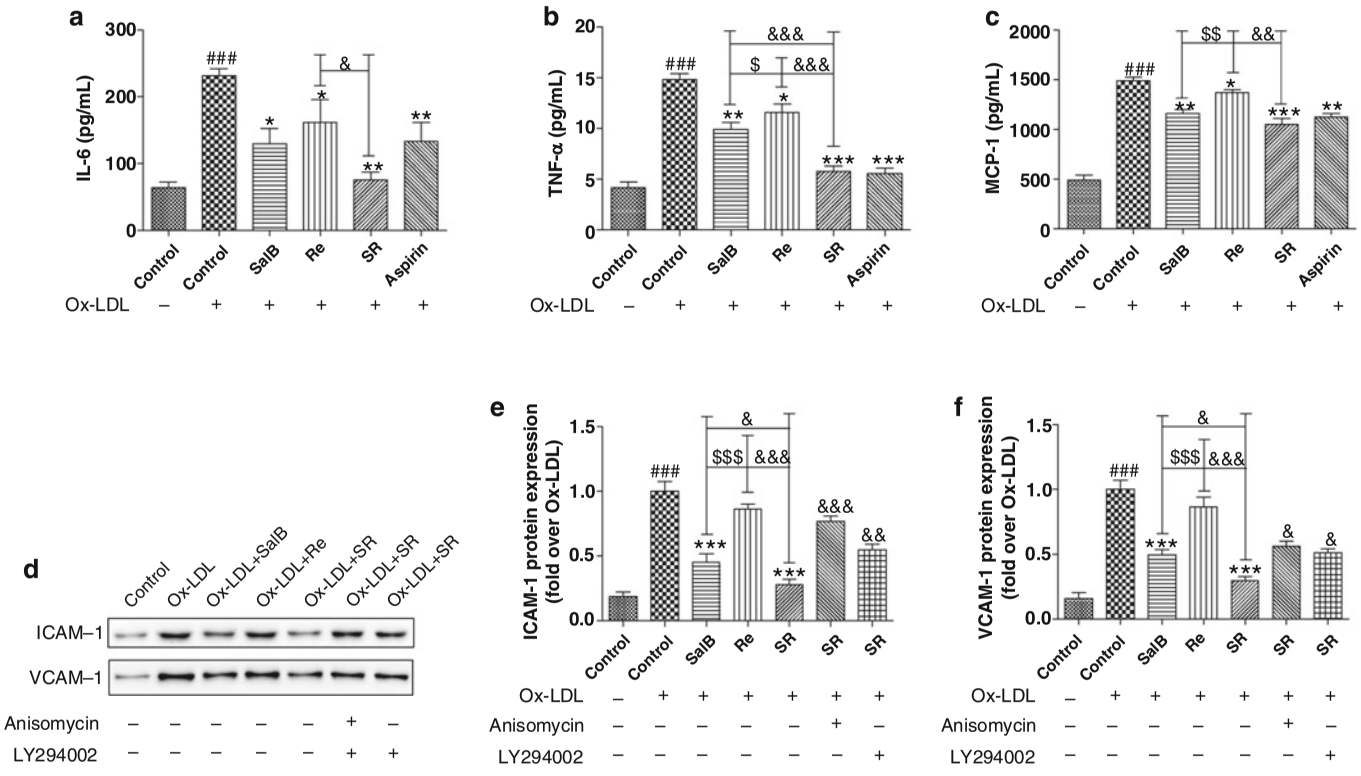

Fig. 7.52 SalB, Re, and SR inhibit the secretion of inflammatory factors in HUVECs induced by Ox-LDL [32]. (**a**) Protective effect of SalB, Re, and SR pre-incubation for 12 h on Ox-LDL-induced over-production in HUVECs IL-6; (**b**) Protective effect of SalB, Re, and SR pre-incubation for 12 h on Ox-LDL-induced over-production in HUVECs TNF-α; (**c**) Protective effect of SalB, Re, and SR pre-incubation for 12 h on Ox-LDL-induced over-production in HUVECs MCP-1; (**d**) effects of pre-incubation with SalB, Re, and SR for 12 h on the expression of ICAM-1 and VCAM-1 in HUVECs induced by Ox-LDL; (**e**) statistical diagram of ICAM-1 expression in HUVECs induced by OX-LDL after pre-incubation with SalB, Re, and SR for 12 h; (*f*) Statistical diagram of VCAM-1 expression in HUVECs induced by OX-LDL after pre-incubation with SalB, Re, and SR for 12 h. $^{***}P < 0.001$, $^{**}P < 0.01$, $^{*}P < 0.05$ compared with Ox-LDL; $^{\#\#\#}P < 0.001$ compared with control; $^{\$\$\$}P < 0.001$, $^{\$\$}P < 0.01$, $^{\$}P < 0.05$ and SalB; $^{\&\&\&}P < 0.001$, $^{\&\&}P < 0.01$, $^{\&}P < 0.05$ compared with SR

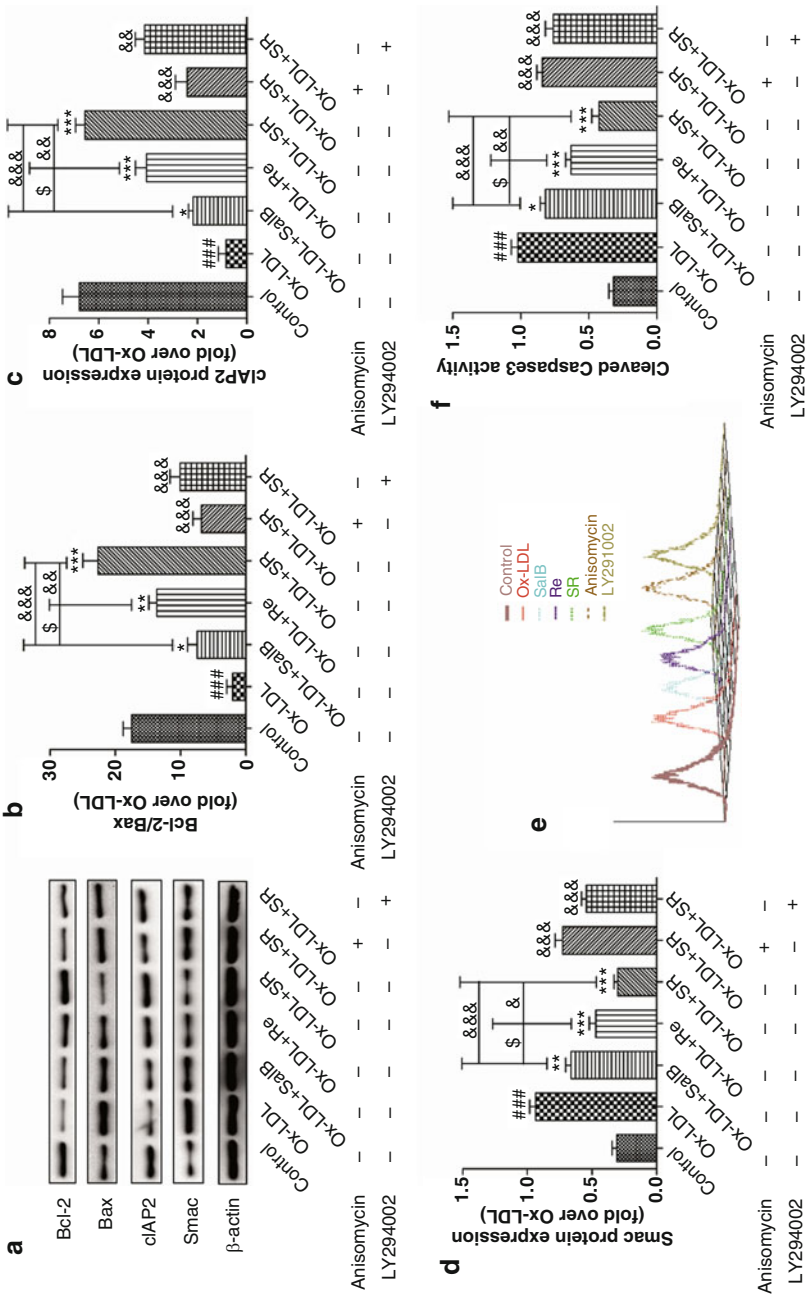

Fig. 7.53 SalB, Re, and SR regulate the expression of apoptosis-related proteins in the damage process of Ox-LDL-induced HUVECs through PI3K/Akt/NF-κB pathway and p38MAPK/NF-κB pathway [32]. (**a**) Regulatory effect of SalB, Re, and SR pre-incubation for 12 h, on the expression of Bcl-2, Bax, cIAP2, and Smac induced by Ox-LDL in HUVECs; (**b**) Statistical diagram of SalB, Re, and SR pre-incubation for 12 h, on the expression of Bcl-2 and Bax induced by

Ox-LDL in HUVECs; (**c**) Statistical diagram of SalB, Re, and SR pre-incubation for 12 h, on the expression of cIAP2 induced by Ox-LDL in HUVECs; (**d**) Statistical diagram of SalB, Re, and SR pre-incubation for 12 h, on the expression of Smac induced by Ox-LDL in HUVECs; (**e**) 3D model diagram of cleaved Caspase3 activity detected by flow cytometry when SalB, Re, and SR are pre-incubated for 12 h, on Ox-LDL-induced HUVECs' injury; (**f**) Statistical diagram of cleaved Caspase3 activity detected by flow cytometry when SalB, Re, and SR are pre-incubated for 12 h, on Ox-LDL-induced HUVECs' injury. $^{***}P < 0.001$, $^{**}P < 0.01$, $^{*}P < 0.05$ compared with Ox-LDL; $^{\#\#\#}P < 0.001$ compared with Control; $^{\$}P < 0.05$ and SalB; $^{\&\&\&}P < 0.001$, $^{\&\&}P < 0.01$, $^{\&}P < 0.05$ compared with SR

7.6.4.4 Summary

This section takes the combined use of salvianolic acid B and ginsenoside Re as an example, to introduce in detail the experimental ideas and procedures for the development of multi-target drugs based on the network pharmacology method, and provides reference for the application of network pharmacology in multi-target drug research. Relying on literature and database retrieval technologies, this section constructs a molecular target network based on the network pharmacology method to protect endothelial cell damage induced by low-density lipoprotein by combining salvianolic acid B and ginsenoside Re, and analyzes the rationality of multi-target drug development based on the combined use of drugs from three different levels, i.e. target, gene ontology, and KEGG pathway. Finally, using oxidative low-density lipoprotein-induced human umbilical cord vein endothelial cell injury as a model, and by adopting relevant effect indicators such as oxidative stress, inflammatory response, and endothelial cell apoptosis, this section verifies the protective effects of salvianolic acid B, ginsenoside Re monomer, and their compatibility on oxidized low-density lipoprotein-induced human umbilical cord vein endothelial cell injury. The results show that salvianolic acid B, ginsenoside Re monomer, and their compatibility play a role in protecting endothelial cells by interfering with the oxidative stress, inflammation, and apoptosis in the process of oxidized low-density lipoprotein-induced human umbilical cord vein endothelial cell injury.

References

1. Zeng K. Modernization research strategy and thinking of complex system of traditional Chinese medicine. Beijing: Science Press; 2016.
2. Guo W. Brief discussion on old and new technology of traditional Chinese medicine extraction process. Chem Pharm Eng. 2005;26(1):41–7.
3. Hopkins AL. Network pharmacology: the next paradigm in drug discovery. Nat Chem Biol. 2008;4(11):682–90.
4. Han B, Huang W, Xie X, et al. Thought and methodology of toxicity-efficacy network integrated analysis of toxic aconitum. World Chin Med. 2017;12(11):2585–97.
5. Tang S, Xing X, Deng X, et al. Research progress of Guanxin Danshen formula and its effective components in treating coronary artery heart disease. J Chin Mater Med. 2016;41(20):3721–6.
6. Xie L, Draizen E, Bourne P. Harnessing big data for systems pharmacology. Annu Rev Pharmacol Toxicol. 2017;57:245–62.
7. Wang J, Liu R, Liu B, et al. Systems pharmacology-based strategy to screen new adjuvant for hepatitis B vaccine from traditional Chinese medicine ophiocordyceps sinensis. Sci Rep. 2017;7:44788.
8. Li Y, Wang J, Xiao Y, et al. A systems pharmacology approach to investigate the mechanisms of action of Semen Strychni and Tripterygium wilfordii Hook F for treatment of rheumatoid arthritis. J Ethnopharmacol. 2015;175(2015):301–14.
9. Sun B, Xiao J, Sun X, et al. Notoginsenoside R1 attenuates cardiac dysfunction in endotoxemic mice: an insight into oestrogen receptor activation and PI3K/Akt signalling. Br J Pharmacol. 2013;168(7):1758–70.

10. Meng X, Sun G, Ye J, et al. Notoginsenoside R1-mediated neuroprotection involves estrogen receptor-dependent crosstalk between Akt and ERK1/2 pathways: a novel mechanism of Nrf2/ARE signaling activation. Free Radic Res. 2014;48(4):445–60.
11. Deng X, Xing X, Sun G, et al. Guanxin Danshen formulation protects against myocardial ischemia reperfusion injury-induced left ventricular remodeling by upregulating estrogen receptor β. Front Pharmacol. 2017;8(2017):777.
12. Goldstein L, Adams R, Alberts M, et al. Primary prevention of ischemic stroke: a guideline from the American Heart Association/American Stroke Association Stroke Council: cosponsored by the Atherosclerotic Peripheral Vascular Disease Interdisciplinary Working Group; Cardiovascular Nursing Council; Clinical Cardiology Council; Nutrition, Physical Activity, and Metabolism Council; and the Quality of Care and Outcomes Research Interdisciplinary Working Group. Stroke. 2006;37(6):1583–633.
13. Donnan G-A, Fisher M, MacLeod M, et al. Stroke. Lancet. 2008;371(9624):1612–23.
14. Lin J, Zhang Y, Cui J, et al. Development status and prospects of the panax notoginseng industry in our country. Chin Pharm. 2005;14(2):18.
15. Yu N. Pharmacological effects of panax notoginseng saponins on cardiovascular system. Zhejiang J Integr Trad Chin West Med. 2000;10(4):66–7.
16. Sun F, Sun M, Lv X. Research progress on the effect of Chinese medicine panax notoginseng on hemostasis and promoting blood circulation. J Med Res. 2013;42(9):24–6.
17. Xie W, Meng X, Zhai Y, et al. Panax notoginseng saponins: a review of its mechanisms of antidepressant or anxiolytic effects and network analysis on phytochemistry and pharmacology. Molecules. 2018;23(4):940.
18. Yang W, Li Y, Sun L, et al. Complex network analysis on dynamic change regularity of combining use of Chinese and western medicine in 27678 cases with ischemic stroke in acute phase. J Chin Mater Med. 2015;40(24):4783–90.
19. Chen L, Chen S, Yang M, et al. Analysis on the clinical value of notoginseng total saponin combined with aspirin in the treatment of cerebral infarction for 120 cases. Chin Med Mod Distance Educ China. 2018;16(10):54–6.
20. Rodrigo R, Fernandez-Gajardo R, Gutierrez R, et al. Oxidative stress and pathophysiology of ischemic stroke: novel therapeutic opportunities. CNS Neurol Disord Drug Targets. 2013;12(5):698–714.
21. Radermacher K, Wingler K, Kleikers P, et al. The 1027th target candidate in stroke: will NADPH oxidase hold up? Exp Transl Stroke Med. 2012;4(1):11.
22. Moskowitz M, Lo E, Iadecola C. The science of stroke: mechanisms in search of treatments. Neuron. 2010;67(2):181–98.
23. Serrano-Pozo A, Frosch M, Masliah E, et al. Neuropathological alterations in Alzheimer disease. Cold Spring Harb Perspect Med. 2011;1(1):6189.
24. Zhou Y, Li HQ, Lu L, et al. Ginsenoside Rg1 provides neuroprotection against blood brain barrier disruption and neurological injury in a rat model of cerebral ischemia/reperfusion through downregulation of aquaporin 4 expression. Phytomedicine. 2014;21(7):998–1003.
25. Taille C, El-Benna J, Lanone S, et al. Induction of heme oxygenase-1 inhibits NAD(P)H oxidase activity by down-regulating cytochrome b558 expression via the reduction of heme availability. J Biol Chem. 2004;279(27):28681–8.
26. Liu WJ, Tang HT, Jia YT, et al. Notoginsenoside r1 attenuates renal ischemia-reperfusion injury in rats. Shock. 2010;34(3):314–20.
27. Wang Y, Tu L, Li Y, et al. Notoginsenoside R1 protects against neonatal cerebral hypoxic-ischemic injury through estrogen receptor-dependent activation of endoplasmic reticulum stress pathways. J Pharmacol Exp Ther. 2016;2016:230359.
28. Wang Y, Tu L, Li Y, et al. Notoginsenoside R1 alleviates oxygen–glucose deprivation/reoxygenation injury by suppressing endoplasmic reticulum calcium release via PLC. Sci Rep. 2017;7(1):16226.
29. Norata GD, Tibolla G, Catapano AL. Statins and skeletal muscles toxicity: from clinical trials to everyday practice. Pharmacol Res. 2014;88:107–13.

30. Hopkins AL. Network pharmacology. Nat Biotechnol. 2007;25(10):1110–1.
31. Zheng F, Guo M, Gu L, et al. Effects of salvianolic acid B on stability of atherosclerotic plaque in apolipoprotein E gene knock-out mice treated with STZ and high fat diet. Chin J Arterioscler. 2011;19(11):885–90.
32. Ke Y, Yun L, Shan L, et al. Salvianolic acid B and ginsenoside Re synergistically protect against Ox-LDL-induced endothelial apoptosis through the antioxidative and antiinflammatory mechanisms. Front Pharmacol. 2018;9:662.
33. Fang F, Qiu L, Miao J, et al. Anti-inflammatory and antioxidant effect of ginsenoside Re on the lung injury induced by intestinal ischemia reperfusion in rats. Central South Pharm. 2014;12 (06):521–4.